

Chapter 20

EMISSIONS CHARACTERISTICS OF HIGHER ALCOHOL/GASOLINE BLENDS

Mridul Gautam and Daniel W. Martin II

Department of Mechanical and Aerospace Engineering
West Virginia University
Morgantown, WV

Abstract

An experimental investigation was conducted to determine the of emission characteristics of higher alcohols and gasoline (UTG96) blends. While lower alcohols (methanol and ethanol) have been used in blends with gasoline, very little work has been done reported on higher alcohols (propanol, butanol, and pentanol).

Comparisons of emissions and fuel characteristics between higher alcohol/gasoline blends and neat gasoline were made to determine the advantages and disadvantages of blending higher alcohols with gasoline. All tests were conducted on a single cylinder Waukesha Cooperative Fuel Research (CFR) engine operating at steady state conditions and stoichiometric A/F ratio. Emissions tests were conducted at the optimum spark timing-knock limiting compression ratio (KLCR) combination for the particular blend being tested. The cycle emissions (mass per unit time; g/hr) of CO, CO₂, and organic matter hydrocarbon equivalent (OMHCE) from the higher alcohol/gasoline blends were very similar those from neat gasoline. Cycle emissions of NO_x from the blends were higher than those from neat gasoline. However, for all the emissions species considered, the brake specific emissions (g/kw-hr) were significantly lower for the higher alcohol/gasoline blends than for neat gasoline. This was due to the fact that the blends had greater resistance to knock and allowed higher compression ratios, which increased engine power output. The contribution of alcohols and aldehydes to the overall OMHCE emissions was found to be minimal.

Cycle fuel consumption (g/hr) of higher alcohol/gasoline blends was slightly higher than neat gasoline due to the lower stoichiometric A/F ratios required by the blends. However, the brake specific fuel consumption (g/kW-hr) for the blends was significantly lower than that for neat gasoline.

Other fuel parameters, including Reid vapor pressure (RVP) and distillation curve, are affected by the addition of alcohol to gasoline. The lower alcohols (methanol and ethanol) cause the most dramatic increase in RVP and the largest depression of the distillation curve. Addition of the higher alcohols (propanol, butanol, and pentanol) seems to curb the effects of methanol and ethanol on both RVP and the distillation curve.

Background

Effect of Alcohol on Blend Vapor Pressure and Evaporative Emissions

Furey (1985) investigated RVP changes in gasoline when methanol, ethanol, and higher alcohols were added. His findings showed that very small amounts of alcohol in the blend drastically increased the RVP, and methanol seemed to have a more dramatic effect on RVP than higher alcohols. This was due to the fact that methanol forms low-boiling azeotropes with certain hydrocarbons. However, when methanol was blended in gasoline along with higher alcohols, the increase in RVP was lower compared to methanol alone. Hence, using higher alcohols as co-solvents in alcohol/gasoline blends seems to be a viable option for controlling RVP and, consequently, for controlling evaporative emissions.

Reddy (1986) compared the evaporative emissions of blends containing three levels of methanol and tertiary butyl alcohol (TBA) with gasolines of closely matched RVP. Three different fuel metering systems were tested: carburetor, throttle body injection (TBI), and multi-port fuel injection (MFI). The alcohol blends generated the same vapor levels as gasolines matched to the same ASTM D 439 volatility.

Although an alcohol/gasoline blend with an RVP close to that of neat gasoline may not produce substantially increased evaporative emissions, mixing an alcohol/gasoline blend with neat gasoline increases the RVP of the mixture. Furey (1987) investigated RVP changes when pure gasoline and an alcohol/gasoline blend of matched RVP were mixed together, as might be the case with an on-the-road vehicle. The results showed that even though a blend may have the same RVP as gasoline, a mixture of the two produces a fuel with a higher RVP. Thus, a vehicle would have to be fueled solely on neat gasoline or an alcohol/gasoline blend of matched RVP in order to avoid an increase in RVP of the tank fuel.

Alcohol Effects on Distillation, Cold Starting, and Vapor Lock

Adding alcohols to gasoline depresses the boiling temperature of individual hydrocarbons. The lower alcohols cause significant reduction in the front end distillation temperatures, thus affecting primarily the first 50% evaporated. Lower molecular weight alcohols have the greatest effect on boiling point depression. In particular, methanol causes the largest changes; its effects can be observed even when accompanied by a co-solvent. Higher molecular weight alcohols, such as Tertiary Butyl Alcohol (TBA), propanol, butanol, and pentanol, exert smaller changes on the distillation characteristics.

Yaccarino (1985) of General Motors Research compared the high temperature [26.7°C - 32.2°C (80°F - 90°F)] driveability and vapor lock performance of methanol blends using six cars with closed-loop fuel control systems: three cars had carburetors, two had throttle body injection, and one car was equipped with multi-port fuel injection. Four blends were tested: 3% methanol, 7% methanol, 4.75% methanol with 4.75% TBA, and 8.2% methanol with 2.7% TBA (all percentages by volume). The blends were matched with two gasolines meeting ASTM specifications for volatility classes C and D, which are fuels designed for typical summer and transitional seasons in the Midwest and Northeastern U.S., respectively. Driveability demerits, which were awarded based on hot engine restart, throttle response, and smoothness of engine performance, were greatest for two of the carbureted cars when alcohol blends were used. The fuel injected cars, and surprisingly one of the carbureted vehicles, performed similarly on the blends and with the gasolines. In the matched volatility vapor lock tests, the carbureted vehicles also performed poorly, with the worst performance on the blends containing the highest methanol concentrations. The poor performance of the carbureted cars, even though they had

closed-loop control, was to be expected with the alcohol blends. This was due to the fact that carburetors operate at very low pressure differentials and are unable to compensate for volume effects of partially vaporized fuel. Fuel injection systems, on the other hand, can deliver fuel to the injectors at pressure as high as 379 KPa (55 psig) and provide much greater tolerance of volatile fuels than is attainable with carbureted systems.

The property of alcohols that reduces cold starting ability the most is their higher (compared with typical gasoline) heat of vaporization. Bardon et al. (1985) investigated engine response to this factor by measuring the mixture richness required for starting between temperatures of -40°C and 15.6°C (-40°F and 60°F). The starting performance of a gasoline with an RVP of 61.4 KPa (8.9 psi) was compared to a blend composed of the same gasoline splash-blended with 10% methanol by volume and an RVP of 80 KPa (11.6 psi). The starting performance was not improved with the high RVP blend and, at stoichiometric mixture ratios for each fuel, gasoline allowed the engine to be started at 5°C (41°F) whereas the blend would not allow starting below 15°C (59°F). A 10% methanol blend matching the 61.4 KPa (8.9 psi) RVP gasoline was also made by removing volatile fractions from the base gasoline. With this blend, the engine would not start at temperatures below 15°C (59°F) unless the mixture strength was enriched about 100% above the stoichiometric A/F of the blend. At -30°C (-22°F), gasoline started the engine with a mixture eight times richer than stoichiometric, but the blend with matched RVP required a mixture strength fourteen times richer than stoichiometric. Rich mixtures are always needed to start cold engines, because enough fuel must vaporize to form a combustible air/fuel mixture. Thus, these studies only demonstrate relative difficulties in starting characteristics, not whether an engine will start when fueled with a blend. The relative cold starting difficulties largely depend on the fuel delivery system. The fuel delivery system must be able to provide a rich enough mixture to allow starting with an alcohol/gasoline blend.

Effects of Alcohol on Stoichiometry, Exhaust Emissions, and Fuel Economy

Alcohol/gasoline blends cause mixture enleanment due to the fact that alcohol requires a lower A/F ratio than gasoline. The leaning effect on the A/F ratio when low levels of oxygenates are used in vehicles without exhaust aftertreatment, results in a reduction both CO and HC emitted exhaust emissions with a slight increase in NO_x . A typical reduction in CO of 30% has been found with a fuel oxygen content of 2% (Mays, 1987). However, if the vehicle is designed to operate close to the lean limit of combustion on hydrocarbon fuels, misfire may occur when oxygenates are present under certain driving regimes with consequent increase in HC emissions (Owen et al., 1995). With vehicles equipped with catalytic converters, the effect of oxygenates found by Mays (1987) indicated reductions in CO and HC and a slight increase in NO_x . These data were obtained using 1978 to 1980 U.S. vehicles and a wide range of oxygenates.

Mixture stoichiometric effects are strongest in vehicles equipped with open-loop fuel metering systems which are calibrated to deliver a set A/F ratio without regard to fuel composition. For those vehicles calibrated richer than stoichiometric, usually older cars, the effect of operating on an alcohol/gasoline blend will be a reduction of CO and HC, and, quite likely, a modest increase in NO_x due to the leaning effect of alcohol on the A/F ratio. For non-catalyst cars with typically lean or near stoichiometric calibrations, operation on an alcohol/gasoline blend could produce a modest reduction in CO but cause the mixture to be sufficiently lean to result in poor combustion and a consequent increase in unburned HC. Catalyst-equipped vehicles with open-loop systems generally show some reduction in CO and HC and small increases in NO_x . Reductions of CO and HC emissions can be observed upstream of the catalyst but are less pronounced after the exhaust passes through a functioning (warmed-

up) catalyst. Changes in the emissions of NO_x , however, can be observed at the tailpipe in vehicles with open-loop systems. In addition, volumetric fuel economy (miles per gallon) is not likely to change in open-loop systems running on alcohol/gasoline blends due to the constant fuel delivery rate (American Petroleum Institute, 1988).

For cars equipped with closed-loop fuel metering systems, which try to keep the mixture near stoichiometric based on a reading from an oxygen sensor in the exhaust, the effect of running on alcohol/gasoline blends will only be noticed when running in open-loop mode. Closed-loop systems run in open-loop mode during warm-up after a cold start and during full power situations. A study by Furey and King (1982) showed that closed-loop systems when running in open-loop mode will show similar trends in exhaust emissions as fully open-loop systems when run on alcohol/gasoline blends. However, when the closed-loop system is functioning, little difference in exhaust emissions is noticed between blends and neat gasoline. As for volumetric fuel economy, closed-loop systems will likely show a decrease because of the capability to compensate for the lower A/F ratio required by alcohol/gasoline blends.

The exhaust from gasoline fueled vehicles commonly contains a spectrum of partially oxidized HC species known as aldehydes. Aldehydes have a very high ozone forming potential, that is, they are highly reactive. For example, formaldehyde and acetaldehyde have high Maximum Incremental Reactivity (MIR) values, 7.009 g $\text{O}_3/\text{g HC}$ and 6.322 g $\text{O}_3/\text{g HC}$, respectively. Acetaldehyde has been shown to produce laryngeal cancers in hamsters and nasal cancers in rats, and formaldehyde is a well-known carcinogen (National Institute for Occupational Safety and Health, 1991). Greater amounts of aldehydes can be generated when alcohol blends are used because the partial oxidation of methanol, ethanol, propanol, butanol, and pentanol directly produces formaldehyde, acetaldehyde, propionaldehyde, butylaldehyde, and pentanaldehyde respectively. Exhaust oxidation catalysts can oxidize most of the aldehydes, and during closed-loop operation, three-way catalysts appear to be even more efficient at eliminating them. Aldehydes that survive the combustion process and the catalytic converter are present in the exhaust in very low concentrations relative to total hydrocarbon concentration levels (Schuetzle et al. 1981).

The Coordinating Research Council (CRC) and the EPA have investigated the trends in aldehyde emissions of alcohol/gasoline blends. In the CRC ethanol blend program (1982), tests of ethanol blends in open-loop cars showed that tailpipe aldehyde emissions averaged 0.012 grams/mile or 50% higher than with gasoline. Aldehyde emissions did not increase significantly in closed-loop vehicles with three-way catalyst technology. In the CRC methanol blend program (1984), no significant difference in aldehyde emissions was observed between any of the blends and gasoline. It is possible that the laboratory procedure used in this program could not accurately measure low levels of aldehyde concentrations. An EPA test program utilizing two 1984 model cars found that aldehyde emissions averaged 0.0043 grams/km (0.108 grains/mile), an increase of 49% over gasoline, when a blend containing 4.5% methanol by volume and 5.7% TBA by volume was used (Gabele et al., 1985). The program identified approximately 80% of the aldehyde increase, or 0.0012 grams/km (0.031 grains/mile), as formaldehyde emissions.

EPA Guidelines for Alcohol/Gasoline Blends

The use of alcohols in unleaded gasoline must be approved by the EPA, which must ensure that emission control systems, currently in place, will not be affected. Thus, there are several EPA guidelines that have to be followed when blending alcohol with gasoline. The “substantially similar” ruling states that alcohol may be added to gasoline provided that the

amount of oxygen in the finished fuel does not exceed 2.7% by mass. However, a number of specific proposals have been granted waivers allowing the use of alcohols in gasoline. The ruling followed throughout this research is the “DuPont Waiver.” Adopted in January 1985, the DuPont Waiver allows for methanol up to 5.0% volume plus at least 2.5% volume co-solvent (ethanol, propanol, butanol, or pentanol) plus corrosion inhibitor, with maximum oxygen content 3.7% by weight.

Test Engine and Blends

Test Engine

The engine used in this research was the ASTM Cooperative Fuel Research engine manufactured by Waukesha Engine Division, Fuel Research Department, Dresser Industries, Waukesha, WI. The complete unit is known as the “ASTM-CFR Engine*.” The Waukesha Engine has been used by several researchers in their investigation of combustion and emissions characteristics of alcohol fuels and blends (Patel et al., 1987; Hunwartzen, 1982; Harrington and Pilot, 1975; Ebersole and Manning, 1972).

The Waukesha Engine is a four stroke, single cylinder, spark ignited, and variable compression ratio engine with specifications listed in Table 1. Engine power absorption and engine motoring capabilities were provided by a 1250 RPM, 3.7 kW (5 HP), 230 V DC dynamometer manufactured by Louis Allis Company, Milwaukee, WI.

Test Blends

Six alcohol/gasoline blends were prepared for this research. As mentioned earlier, these blends followed the EPA DuPont Waiver for alcohol/gasoline blends. Each blend contained 90% (vol) Unleaded Test Gas 96 (UTG 96) from Phillips 66, and 10% (vol) alcohol. The alcohol portion of the blends contained methanol, ethanol, propanol, butanol, and pentanol (see Table 3.2 for properties of the individual alcohols and UTG 96). The concentrations of the individual alcohols were varied while keeping the total alcohol concentration the same. This was done so that the effect of the individual alcohols, not the total alcohol, could be investigated. In order to decide on the concentrations of the various alcohols in the test blends, extensive tables were made which varied the concentrations of the different alcohols while keeping the total O₂ less than 3.7% by weight. Table 3 lists the volumetric composition and oxygen content of the six test blends. In addition, the net heat of combustion for each of the six test blends is given in Table 4.

* The “ASTM-CFR Engine” is also known as the “Waukesha CFR Engine” or simply the “Waukesha Engine”

| | |
|------------------------------------------|--------------------------------------------------------------------------------------------------|
| Type | Water cooled-4 cycle |
| Bore and Stroke | 8.26 cm x 11.43 cm (3.250 in x 4.500 in) |
| Cylinder Swept Volume | 611.7 cm ³ (37.331 in ³) |
| Compression Ratio | 4 to 16 |
| Combustion Chamber Volume (at TDC) | 176.7 cm ³ to 40.8 cm ³ (10.784 in ³ to 2.489 in ³) |
| Connecting Rod Length (center-to-center) | 25.40 cm (10.000 in) |
| Piston Rings (number) | 5 total (4 compression, 1 oil control) |
| Ignition System | Spark (coil-points-Champion D16 spark plug) |
| Weight of Engine (approximate) | 399 kg (880 lb) |
| Weight of Complete Unit (approximate) | 1247 kg (2750 lb) |

Table 1 - Waukesha Engine Specifications

| Property | UTG 96 | Methanol | Ethanol | Propanol | Butanol | Pentanol |
|--------------------------------------|------------------------------------------|--------------------|----------------------------------|----------------------------------|----------------------------------|-----------------------------------|
| Chemical Formula | C ₉ H ₁₈ (Typical) | CH ₃ OH | C ₂ H ₅ OH | C ₃ H ₇ OH | C ₄ H ₉ OH | C ₅ H ₁₁ OH |
| Molecular Weight | 111.21 | 32.04 | 46.07 | 60.10 | 74.12 | 88.15 |
| Oxygen Content, wt. % | 0.00 | 49.93 | 34.73 | 26.62 | 21.59 | 18.15 |
| Stoichiometric A/F | 14.51 | 6.43 | 8.94 | 10.28 | 11.12 | 11.68 |
| Specific Gravity | 0.7430 | 0.7913 | 0.7894 | 0.8037 | 0.8097 | 0.8148 |
| Boiling Point, °C (°F) | 34-207 (94-405) | 65 (149) | 78.3 (173) | 82.2 (180) | 82.7 (181) | — |
| RVP, KPa (psi) | 61.4 (8.9) | 32.4 (4.7) | 19.3 (2.8) | 9.0 (1.3) | 18.6 (2.7) | — |
| Net Ht. of Comb., kJ/L (BTU/gal) | 31,913 (114,500) | 15,887 (57,000) | 21,183 (76,000) | 23,970 (86,000) | 25,921 (93,000) | 26,200 (94,000) |
| Lat. Ht. of Vaporiz., kJ/L (BTU/gal) | 223 (800) | 920 (3,300) | 725 (2,600) | 585 (2,100) | 474 (1,700) | 251 (900) |
| RON | 96.5 | 112 | 111 | 112 | 113 | — |
| MON | 87.2 | 91 | 92 | — | — | — |

Table 2 - Properties of Pure Alcohols and UTG 96 (Bata et al., 1989; Dorn et al., 1986; Dean, 1992; and Phillips 66, 1995)

| Blend No | Volume Percentage of | | | | | | % Volume Alcohols | % wt. Oxygen in Blend |
|----------|----------------------|----------|---------|----------|---------|----------|-------------------|-----------------------|
| | UTG 96 | Methanol | Ethanol | Propanol | Butanol | Pentanol | | |
| 1 | 90.00% | 0.60% | 2.07% | 4.80% | 2.40% | 0.13% | 10.00% | 3.03% |
| 2 | 90.00% | 0.60% | 0.22% | 4.80% | 2.40% | 1.98% | 10.00% | 2.72% |
| 3 | 90.00% | 2.00% | 2.00% | 3.00% | 2.88% | 0.12% | 10.00% | 3.34% |
| 4 | 90.00% | 2.00% | 2.00% | 3.00% | 0.12% | 2.88% | 10.00% | 3.24% |
| 5 | 90.00% | 3.24% | 2.40% | 2.76% | 0.13% | 1.47% | 10.00% | 3.70% |
| 6 | 90.00% | 3.04% | 2.40% | 2.96% | 1.47% | 0.13% | 10.00% | 3.70% |

Table 3 - Volumetric Composition and Oxygen Content of the Test Blends

| Blend ID | kJ/kg | BTU/lb |
|----------|-------|--------|
| UTG 96 | 42912 | 18448 |
| Blend 1 | 42751 | 18379 |
| Blend 2 | 42744 | 18376 |
| Blend 3 | 42779 | 18391 |
| Blend 4 | 42798 | 18399 |
| Blend 5 | 42828 | 18412 |
| Blend 6 | 42821 | 18409 |

Table 4 - Net Heat of Combustion of the Six Test Blends and UTG 96

Instrumentation

Overview

Figure 1 shows a schematic of the CFR engine test bed and all the instrumentation that was installed on the engine. Prior to conducting emission tests steps were taken to ensure that the engine was operating within normal limits and the repeatability of the engine operating conditions from test to test was established. The voltage output from the sensors was related to corresponding engineering parameters via calibration data. Some of the sensors required an “excitation” voltage, so a system of power supplies was constructed to provide the necessary power for the sensors. A 5-volt, a 10-volt, and a 15-volt power supply were used in the power system. Once all the sensors were installed, the voltages output by the sensors were read by an A/D data acquisition board installed in an IBM PC driven by a BASIC 7 program.

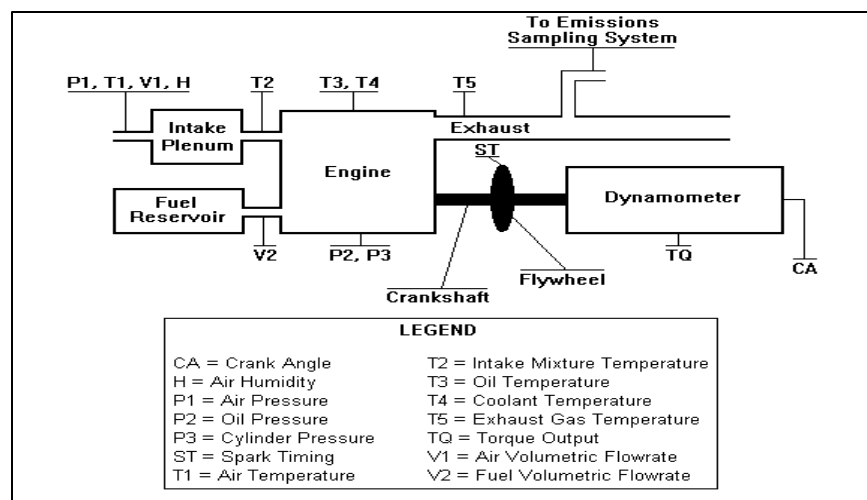


Figure 1 - Schematic of Waukesha Engine Instrumentation

Exhaust Emissions Sampling System

An exhaust emissions sampling system based on a micro-dilution tunnel (Gautam, 1994), was constructed to measure the mass emission rates of exhaust species under consideration. The system pulled raw exhaust from the exhaust pipe, through a heated line, into a heated dilution chamber. Inside the dilution chamber, the exhaust was mixed with metered zero humidity air from an air cylinder. Diluting the raw exhaust lowered the dew point temperature sufficiently to prevent water or alcohol condensation. After dilution, the exhaust was diverted into three separate lines. The first line directed a sample of the diluted exhaust to a bag which was later analyzed for CO, CO₂ and NO_x on an exhaust analysis bench in the West Virginia University's Engine Research Center. CO and CO₂ were analyzed using Rosemount Model 868 Non-dispersive Infrared (NDIR) analyzers. NO_x was analyzed on Rosemount Model 955 heated chemiluminescent analyzer. The second line led the diluted exhaust through a set of two bubblers filled with de-ionized water. Any unburned alcohol in the diluted exhaust dissolved in the bubbler water. After a test, the contents of the bubblers were analyzed for alcohols on a flame ionization detector (FID) gas chromatograph (GC). The third line directed the diluted exhaust through a DNPH (2,4-dinitrophenylhydrazine) coated silica gel cartridge. The aldehydes

in the exhaust reacted with the DNPH in the cartridge to form stable hydrazone derivatives, which were later eluted and analyzed using high performance liquid chromatography (HPLC). The analysis of the DNPH cartridges was performed by Atmospheric Analysis & Consulting, Inc., 4572 Telephone Road, Ventura, California. In addition to capturing diluted exhaust samples, the exhaust sampling system also included an in-line heated flame ionization detector (HFID) for continuous measurement of unburned HC.

The exhaust sampling system used a set of three-way valves for directing the diluted exhaust flow. The system could be operated in two distinct modes. The first mode was the warm-up/bypass mode which conditioned the lines and the dilution chamber with exhaust before any samples were drawn. The second mode was the sample mode where the diluted exhaust flows were diverted through the bubblers, through the DNPH cartridge, and into the bag. Figure 2 shows the sampling system in warm-up/bypass mode and Figure 3 shows the system in sample mode.

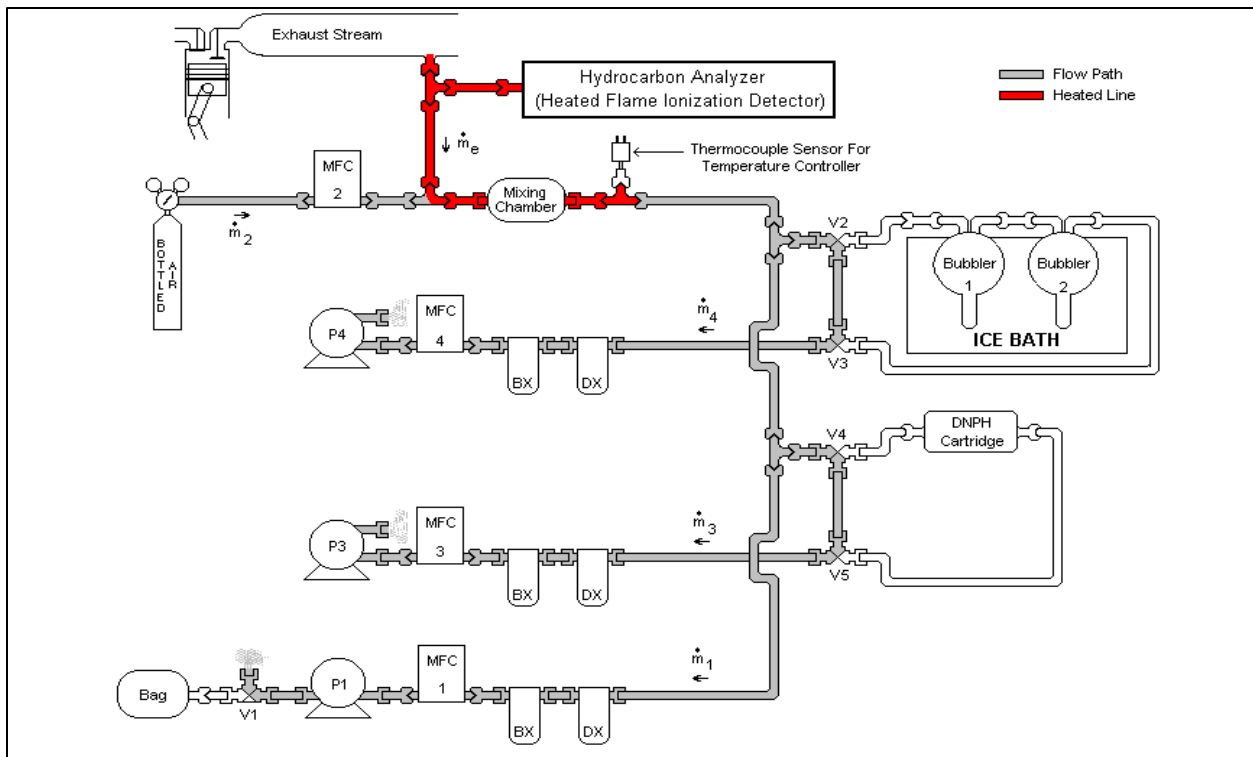


Figure 2 - Exhaust Emissions Sampling System in Warm-Up/Bypass Mode

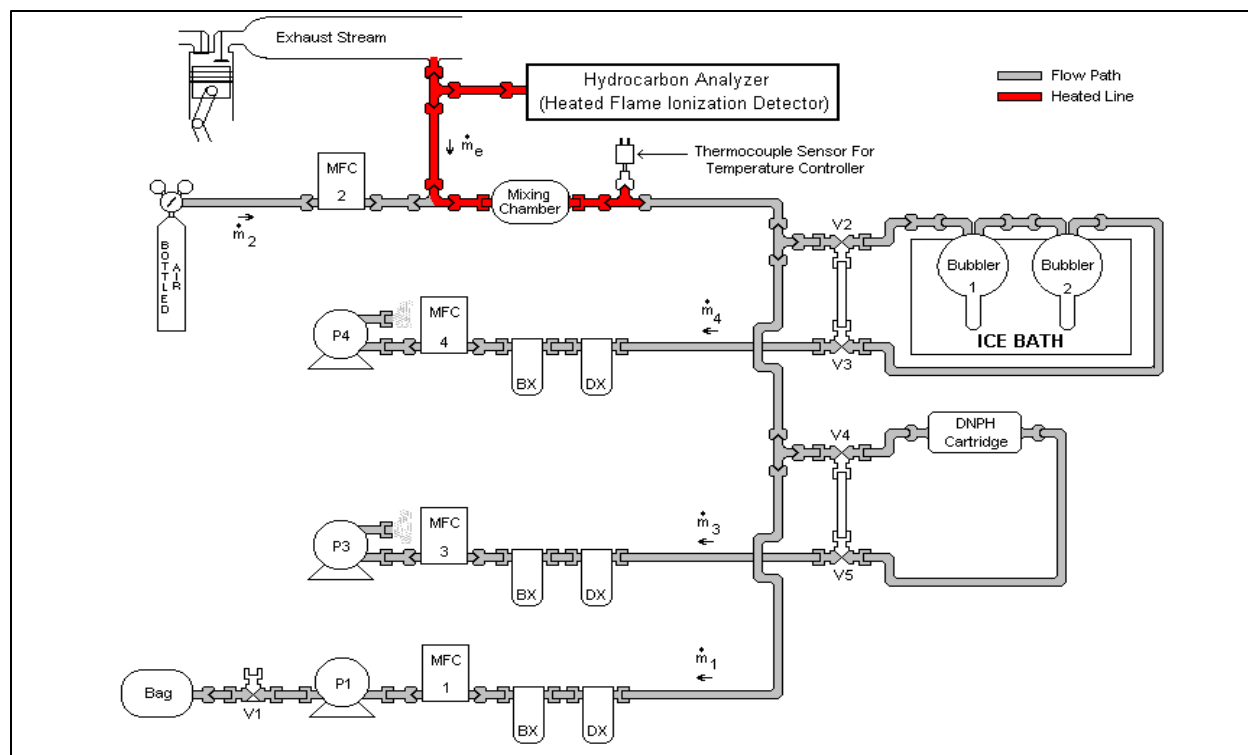


Figure 3 - Exhaust Emissions Sampling System in Sample Mode

The flowrates through the various lines in the exhaust emissions sampling system were controlled by a set of four mass flow controllers (MFCs) from Seirra Instruments, Inc. In order to protect the internal components of the MFCs, a set of two filters was installed on each line. These filters labeled “DX” and “BX” are Balston® coalescing filters which remove 99.99% of particles and mist from air and other gases.

The sampling lines used in the exhaust emissions sampling system were 6.35-mm (0.250-inch) OD, 0.89-mm (0.035-inch) wall stainless steel tubing. In addition, the valves, fittings, MFC bodies, and filter bodies were also made of stainless steel.

Data Acquisition

Overview

An RTI-835L data acquisition board from Analog Devices, which has 16 analog input channels and two digital I/O channels, was used to interface all the transducers with a dedicated computer. The board was driven by means of data acquisition software developed in BASIC 7. The board was also capable of timing analog input operations with external events via triggering and pacing. The software used for driving the RTI-835L board employed a BASIC 7 software package from Analog Devices.

Engine Operating Conditions and Emissions

The voltage signals from various transducers monitoring the engine operating conditions were supplied to the data acquisition board via the analog input channels. One exception was the engine speed. Engine speed was monitored by measuring the frequency of the square wave

coming from the crankshaft encoder. The data acquisition board has a counter/timer channel, which was part of the digital I/O section of the board, that could be set up to measure the frequency of an incoming signal. Once the transducers were wired into the data acquisition board, the appropriate subroutines were called from the software package to read the voltages and frequencies coming from the sensors. The calibration information was programmed into the software so that the incoming voltages and frequencies could be converted into corresponding engineering parameters.

The engine operating conditions were monitored and recorded during the blend testing program. In addition to the engine performance data, HC emissions measured by the in-line HFID were also recorded and archived. The other emissions species (CO, CO₂, and NO_x) were analyzed from the bag sample captured by the emissions sampling system.

Other Blend Properties

These blend properties included the ASTM D-86 distillation curves, hydrocarbon types, net heat of combustion, Reid vapor pressure, research octane number, and motor octane number. These blend parameters were reported by Core Laboratories. Data obtained from Core Laboratories was assured to be in compliance with NIST standards and test procedures.

Data Analysis

Calculation of Mass Emission Rates from Diluted Exhaust Analysis

Mass emission rates were calculated from the diluted exhaust analysis by using the following equation (for a detailed derivation, refer to Martin II, 1997)

$$\dot{m}_E^i = 3.6 \times 10^{-3} \frac{(\dot{m}_A + \dot{m}_F) M_i}{M_E} \left[C_{DE}^i + \mathbf{d} (C_{DE}^i - C_{DA}^i) \right] \quad (1)$$

Where:

- \dot{m}_E^i = mass emission rate of constituent i from the engine (g/hr)
- \dot{m}_A = mass flowrate of air into the engine (g/s)
- \dot{m}_F = mass flowrate of fuel into the engine (g/s)
- M_i = molecular weight of constituent i (g/gmol)
- M_E = molecular weight of raw exhaust (g/gmol)
- C_{DE}^i = concentration of constituent i in the diluted exhaust (ppm)
- C_{DA}^i = concentration of constituent i in the dilution air (ppm)
- $\mathbf{d} = \frac{\dot{V}_{DA}}{\dot{V}_{RE}} = \frac{\text{standard volume flowrate of dilution air}}{\text{standard volume flowrate of raw exhaust into sampling system}}$

Mass emission rates are usually specified in $\frac{\text{grams}}{\text{kW} \cdot \text{hr}}$ or $\frac{\text{lb}}{\text{HP} \cdot \text{hr}}$. Thus, dividing the right hand side of Eq. 1 by the engine power output, \dot{W} , yields:

$$\dot{m}_E^i = 3.6 \times 10^{-3} \frac{(\dot{m}_A + \dot{m}_F) M_i}{\dot{W} M_E} \left[C_{DE}^i + \mathbf{d} (C_{DE}^i - C_{DA}^i) \right] \quad (2)$$

\dot{m}_E^i calculated from Eq. 2 is expressed in terms of $\frac{\text{grams}}{\text{kW} \cdot \text{hr}}$ when \dot{W} is in kW and the other parameters have the units specified in Eq. 1.

CO, CO₂, and NO_x Emissions

The concentrations of CO, CO₂, and NO_x in the diluted exhaust were measured by non-dispersive infrared analyzers (CO and CO₂) and a chemiluminescent analyzer (NO_x), respectively. The mass emission rates of these constituents were calculated directly from Equations 1 and 2. However, a humidity correction factor, K_H was included in the NO_x mass emission rate calculations:

$$K_H = \frac{1}{1 - 0.0047 \left(\frac{43.478 R_i P_d}{P_B - \left(P_d \frac{R_i}{100} \right)} - 75 \right)} \quad (3)$$

Where: R_i = relative humidity of the engine intake air, in percent

P_d = Saturated vapor pressure at the engine intake air dry bulb temperature

P_B = Barometric pressure

The NO_x emission rate obtained from Eq. 1 or Eq. 2 was multiplied by K_H (from Equation 3) to get the corrected NO_x emissions.

Unburned Alcohol Emissions

The unburned alcohol emissions were captured in the water bubblers of the emissions sampling system and were calculated from the following equation (for a detailed derivation, refer to Martin II, 1997)

$$C_{DE}^k = 8.205 \times 10^{-2} \frac{\rho_L^k V_B (C_{B1}^k + C_{B2}^k) T}{M_k P \dot{V}_{DE}^B t} \quad (4)$$

Where: C_{DE}^k = concentration of alcohol k in the diluted exhaust (ppm)

ρ_L^k = density of liquid alcohol k (g/cm³)

V_B = volume of water in each bubbler (cm³)

C_{B1}^k = concentration of liquid alcohol k in bubbler #1 (ppm)

C_{B2}^k = concentration of liquid alcohol k in bubbler #2 (ppm)

T = standard temperature set in mass flow controllers (°K)

M_k = molecular weight of alcohol k (g/gmol)

P = standard pressure set in mass flow controllers (atm)

\dot{V}_{DE}^B = standard volume flowrate of diluted exhaust through bubblers (L/min)

t = amount of time exhaust sampling took place (min)

The concentration of alcohol k in the diluted exhaust calculated from Eq. 4 was substituted into either Eq. 1 or Eq. 2 to get the mass emission rate of alcohol k .

Aldehyde Emissions

Aldehyde emissions (formaldehyde, acetaldehyde, propionaldehyde, butylaldehyde, and pentanaldehyde) were captured in the 2,4-DNPH cartridge in the emissions sampling system.

The amount of the particular aldehyde captured in the DNPH cartridge was reported in **mg** from analysis of the cartridge by another commercial analytical laboratory (Atmospheric Analysis & Consulting). Equation 5 was used to calculate aldehyde emissions (for a detailed derivation, refer to Martin II, 1997).

$$C_{DE}^k = 8.205 \times 10^{-8} \frac{m^k T}{M_k P \dot{V}_{DE}^{DNPH} t} \quad (5)$$

Where:

- C_{DE}^k = concentration of aldehyde k in the diluted exhaust (ppm)
- m^k = mass of aldehyde k captured in the DNPH cartridge (**mg**)
- T = standard temperature set in mass flow controllers ($^{\circ}\text{K}$)
- M_k = molecular weight of aldehyde k (g/gmol)
- P = standard pressure set in mass flow controllers (atm)
- \dot{V}_{DE}^{DNPH} = standard volume flowrate of diluted exhaust through the DNPH cartridge (L/min)
- t = amount of time exhaust sampling took place (min)

Like the unburned alcohol concentration calculated from Eq. 4, the aldehyde concentration in the diluted exhaust calculated from Eq. 5 is substituted into either Eq. 1 or Eq. 2 to get the mass emission rate of aldehyde k .

HC Emissions

Total HC concentration was measured with an in-line heated flame ionization detector (HFID). Hydrocarbons measured by the HFID and not measured as unburned alcohols are reported as RHC (Residual Hydrocarbons). RHC is calculated from the following (Code of Federal Regulations, 1994):

$$\text{RHC} = \text{HFID} - \sum_i r_i C_i \quad (6)$$

where r_i are the HFID response factors for the particular alcohol, and C_i are the concentrations of the particular alcohol in the exhaust. The alcohol response factors were determined by analyzing a known concentration of a particular alcohol using the HFID (calibrated on propane). Hence:

$$r = \frac{\text{HFID reading in ppm}}{\text{Alcohol concentration in mixture, ppm}} \quad (7)$$

The values obtained for the response factors of the HFID to each alcohol are listed in Table 5.

| Alcohol | HFID Response Factor |
|----------|----------------------|
| Methanol | 0.5849 |
| Ethanol | 0.6322 |
| Propanol | 0.6345 |
| Butanol | 0.6387 |
| Pentanol | 0.6412 |

Table 5 - HFID Response Factors to Alcohols

Since the HC concentration is measured directly from the raw exhaust by the in-line HFID, there is no need to calculate the HC concentration in the raw exhaust. Thus, the $\left[C_{DE}^i + d(C_{DE}^i - C_{DA}^i) \right]$ term in Equations 1 and 2 can be replaced by the RHC reading (in ppm) from the HFID.

Organic Matter Hydrocarbon Equivalent

Organic Matter Hydrocarbon Equivalent (OMHCE) is commonly used to denote the total hydrocarbon mass emitted from the engine as unburned and partially burned fuel. For a fuel blend containing alcohols, the OMHCE is:

$$\begin{aligned} \text{OMHCE} = \text{RHC} &+ \frac{13.8756}{32.0420} m_{\text{CH}_3\text{OH}} + \frac{13.8756}{23.0344} m_{\text{C}_2\text{H}_5\text{OH}} + \frac{13.8756}{20.0319} m_{\text{C}_3\text{H}_7\text{OH}} + \frac{13.8756}{18.5306} m_{\text{C}_4\text{H}_9\text{OH}} \\ &+ \frac{13.8756}{17.6298} m_{\text{C}_5\text{H}_{11}\text{OH}} + \frac{13.8756}{30.0262} m_{\text{HCHO}} + \frac{13.8756}{22.0265} m_{\text{CH}_3\text{CHO}} + \frac{13.8756}{19.3599} m_{\text{C}_2\text{H}_5\text{CHO}} \\ &+ \frac{13.8756}{18.0267} m_{\text{C}_3\text{H}_7\text{CHO}} + \frac{13.8756}{17.2267} m_{\text{C}_4\text{H}_9\text{CHO}} \end{aligned} \quad (8)$$

Where: RHC = Residual Hydrocarbons calculated from Eq. 6
 m 's are mass emission of the particular constituents from Eq. 1 or Eq. 2
 13.8756 = molecular weight of UTG 96 per carbon atom
 32.0420 = molecular weight of CH_3OH (methanol) per carbon atom
 23.0344 = molecular weight of $\text{C}_2\text{H}_5\text{OH}$ (ethanol) per carbon atom
 20.0319 = molecular weight of $\text{C}_3\text{H}_7\text{OH}$ (propanol) per carbon atom
 18.5306 = molecular weight of $\text{C}_4\text{H}_9\text{OH}$ (butanol) per carbon atom
 17.6298 = molecular weight of $\text{C}_5\text{H}_{11}\text{OH}$ (pentanol) per carbon atom
 32.0262 = molecular weight of HCHO (formaldehyde) per carbon atom
 22.0265 = molecular weight of CH_3CHO (acetaldehyde) per carbon atom
 19.3599 = molecular weight of $\text{C}_2\text{H}_5\text{CHO}$ (propionaldehyde) per carbon atom
 18.0267 = molecular weight of $\text{C}_3\text{H}_7\text{CHO}$ (butylaldehyde) per carbon atom
 17.2267 = molecular weight of $\text{C}_4\text{H}_9\text{CHO}$ (pentanaldehyde) per carbon atom

Results and Discussion

Overview

Since the objective of this study was to evaluate the emissions characteristics of higher alcohol/gasoline blends and compare those characteristics to neat gasoline, it was decided to operate the engine at steady state with certain engine operating conditions held constant. In this manner, combustion and emissions characteristics were dependent on the fuel used in the engine tests and not the engine itself. Table 6 lists the engine operating conditions used in this work.

| Engine Parameter | Specification |
|-----------------------------|-------------------------------------------------------------------------------------|
| Speed | 895 - 905 RPM |
| Intake Manifold Temperature | 45 ^o C - 47.2 ^o C (113 ^o F - 117 ^o F) |
| Crankcase Oil Temperature | 64.4 ^o C - 67.8 ^o C (148 ^o F - 154 ^o F) |
| Coolant Water Temperature | 97.2 ^o C - 98.3 ^o C (207 ^o F - 209 ^o F) |
| Air / Fuel Ratio | Stoichiometric |

Table 6 - Engine Operating Conditions During Blend Testing

For each blend tested, the spark timing-compression ratio combination that produced the best Indicated mean effective pressure (IMEP) was found. Indicated mean effective pressure (IMEP) is a measure of the work done by the gas on the piston per unit volume of the cylinder per mechanical cycle. This allows for the comparison of engines of different sizes, because the size of the engine is scaled out. IMEP is calculated by integrating the pressure-volume curve inside the cylinder and dividing by the cylinder swept volume. Combustion characteristics (including measurement of in-cylinder pressures) of higher alcohols are discussed elsewhere (Gautam and Martin II, 1998).

Once the best IMEP point was found, the emissions tests were conducted at the ignition timing-KLCR (Knock limited compression ratio) combination that produced the best IMEP. KLCR is defined here as the maximum compression ratio at a given ignition timing where the engine will operate without excessive knock. To determine whether or not the engine was knocking excessively, the pressure history inside the cylinder was used. Since the KLCR is a function of ignition timing, the testing procedure consisted of capturing cylinder pressure traces at various ignition timings and compression ratios. Ignition timing was varied between 30^o BTDC and 0^o in increments of 2.5^o. The reason for doing this was that the point of best IMEP is also the point of maximum engine power. Thus, the engine emissions were being compared when the engine spark timing and compression ratio were optimized for a particular blend. Table 7 lists the settings for best IMEP for each blend that were determined prior to conducting emissions tests (Martin II, 1997).

| Blend ID | Spark Timing @Best IMEP | Compression Ratio @ Best IMEP | Best IMEP KPa (psi) |
|----------|-------------------------|-------------------------------|---------------------|
| UTG 96 | -5.0 | 8.8 | 275.9 (40.01) |
| 1 | -5.0 | 9.5 | 337.1 (48.89) |
| 2 | -5.0 | 9.4 | 338.1 (49.04) |
| 3 | -5.0 | 9.9 | 355.1 (51.50) |
| 4 | -5.0 | 9.4 | 338.7 (49.13) |
| 5 | -5.0 | 9.9 | 358.7 (52.02) |
| 6 | -5.0 | 9.9 | 356.9 (51.76) |

Table 7 - Engine Settings for Best IMEP for Each Blend and UTG 96

Emissions and Fuel Consumption

Exhaust samples were collected for emissions analysis at the spark timing-KLRCR values where the engine produced the most power. The power output of the engine at the optimum settings is given in Figure 4 for each blend and UTG 96. Mass emission rates for CO, CO₂, and NO_x are given in Figures 6 - 14; unburned alcohol and partially burned alcohol emissions are given in Figures 17 - 21; and hydrocarbon emissions are given in Figures 22 - 28. Emissions are given in terms of both mass per unit time $\left(\frac{\text{g}}{\text{hr}}, \left(\frac{\text{lb}}{\text{hr}}\right)\right)$ and mass per unit time per unit power output $\left(\frac{\text{g}}{\text{kW} \cdot \text{hr}}, \left(\frac{\text{lb}}{\text{HP} \cdot \text{hr}}\right)\right)$. Throughout the rest of the following discussion, emissions in terms of mass per unit time will be called the cycle emissions, and emissions in terms of mass per unit time per unit power output will be called the brake specific emissions.

Cycle emissions of CO and CO₂ for each blend were almost identical to UTG 96 (within 5% of each other), but the brake specific emissions of CO and CO₂ for the blends were 16% to 23% lower than UTG 96. This can be seen in Figures 6 - 11. Cycle emissions of NO_x from the blends were 12% to 16% higher than UTG 96, but the brake specific emissions of NO_x from the blends were between 5% and 11% lower than UTG 96 (see Figures 12 - 14). The higher cycle emissions of NO_x from the blends may have resulted due to higher in-cylinder temperatures. Figure 15 shows the temperatures at the exhaust port of the engine during emissions testing for each blend and UTG 96. As can be seen, the exhaust temperatures for the blends were higher than UTG 96.

Cycle emissions of alcohols and aldehydes are shown in Figures 17 - 21. These emissions were very low. All alcohol emissions were on the order of $1 \times 10^{-2} \frac{\text{g}}{\text{hr}}$ and aldehyde emissions were on the order of $1 \times 10^{-8} \frac{\text{g}}{\text{hr}}$. The alcohol emissions followed the expected trend. For each alcohol, the volume percentage in the blends is presented along with the emissions levels in Figures 17 - 21. The more of a particular alcohol there was in the blend, the higher were the emissions of that unburned alcohol. Formaldehyde emissions were virtually the same for all the blends, but formaldehyde can be formed from combustion of any of the alcohols. Acetaldehyde may only be formed from combustion of ethanol and higher alcohols. Propionaldehyde can only be formed from combustion of propanol and higher alcohols, and so on. As the order of the aldehyde got higher, the emissions of that particular aldehyde became more influenced by the concentration of the corresponding (same C number) alcohol in the fuel. In the case of pentanaldehyde, the emissions followed the exact trend of the pentanol concentration in the blend because pentanaldehyde can only be formed from combustion of pentanol.

HC emissions are reported in terms of the residual hydrocarbons (RHC) and the organic matter hydrocarbon equivalent (OMHCE). RHC emissions originate from the gasoline components of the fuel, and OMHCE emissions take into consideration both the gasoline components and alcohols/aldehydes. RHC emissions are given in Figures 22 - 24 and OMHCE emissions are given in Figures 25 - 27. The cycle emissions of RHC and OMHCE from the blends were within 3% of UTG 96. Had alcohols and aldehydes made up a more significant portion of the total HC emissions, the RHC emissions for the blends would have been lower than UTG 96. Similar to other emissions species, the brake specific emissions of RHC and OMHCE from the blends were quite a bit lower than UTG 96, ranging from 17% to 23% lower. To

determine the contribution of alcohols and aldehydes to the OMHCE emissions, the percentage of OMHCE emissions due to alcohols and aldehydes was calculated and is presented in Figure 28. For every blend, less than 1% of the OMHCE emissions were caused by alcohols and aldehydes.

Fuel consumption rates for the blends and UTG 96 are given in Figures 29 - 31. As expected, the cycle fuel consumption rates of the blends were 1.2% to 3.5% higher than UTG 96 due to the lower A/F ratios required by the blends. However, the brake specific fuel consumption (BSFC) of the blends ranged from 17% to 21% lower than UTG 96 due to the increased engine power output from the blends.

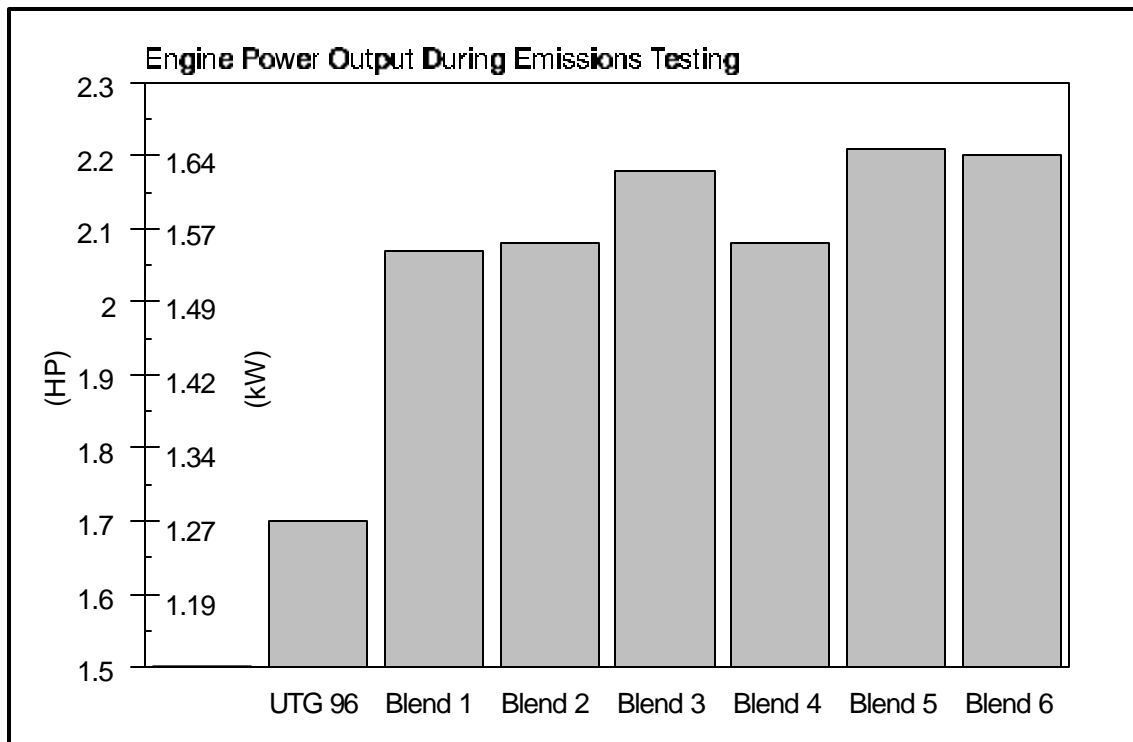


Figure 4 - Engine Power Output During Emissions Testing

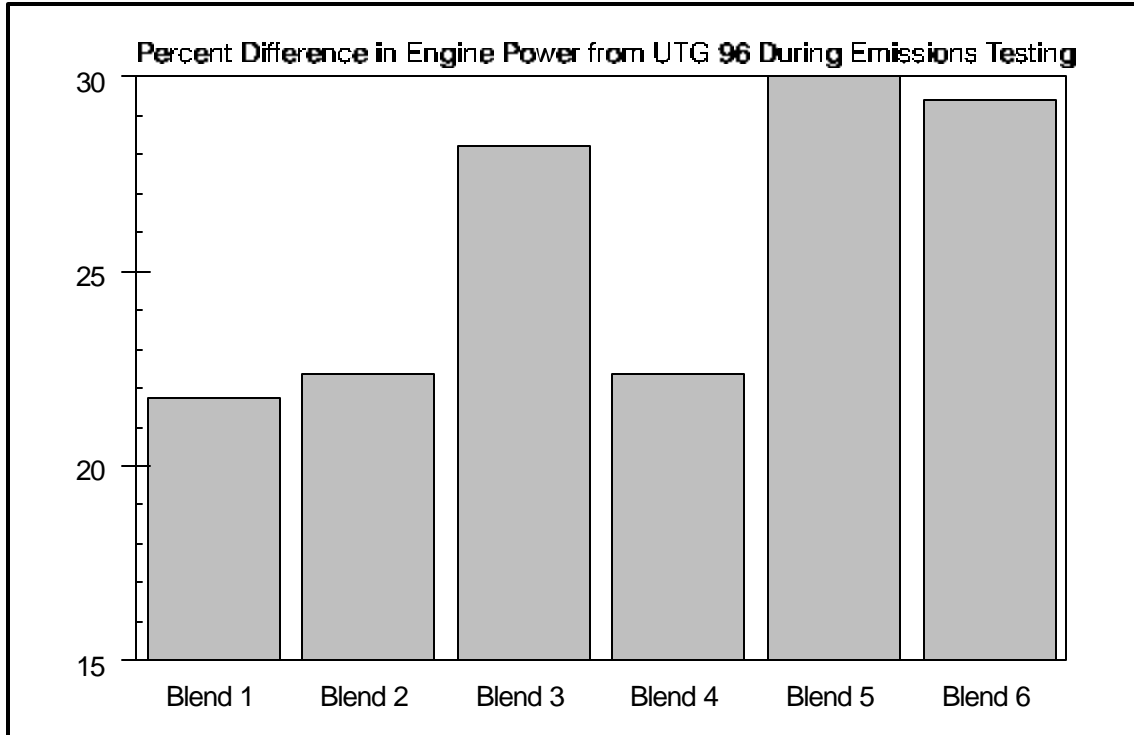


Figure 5 - Percent Difference in Engine Power Output from UTG 96 During Emissions Testing

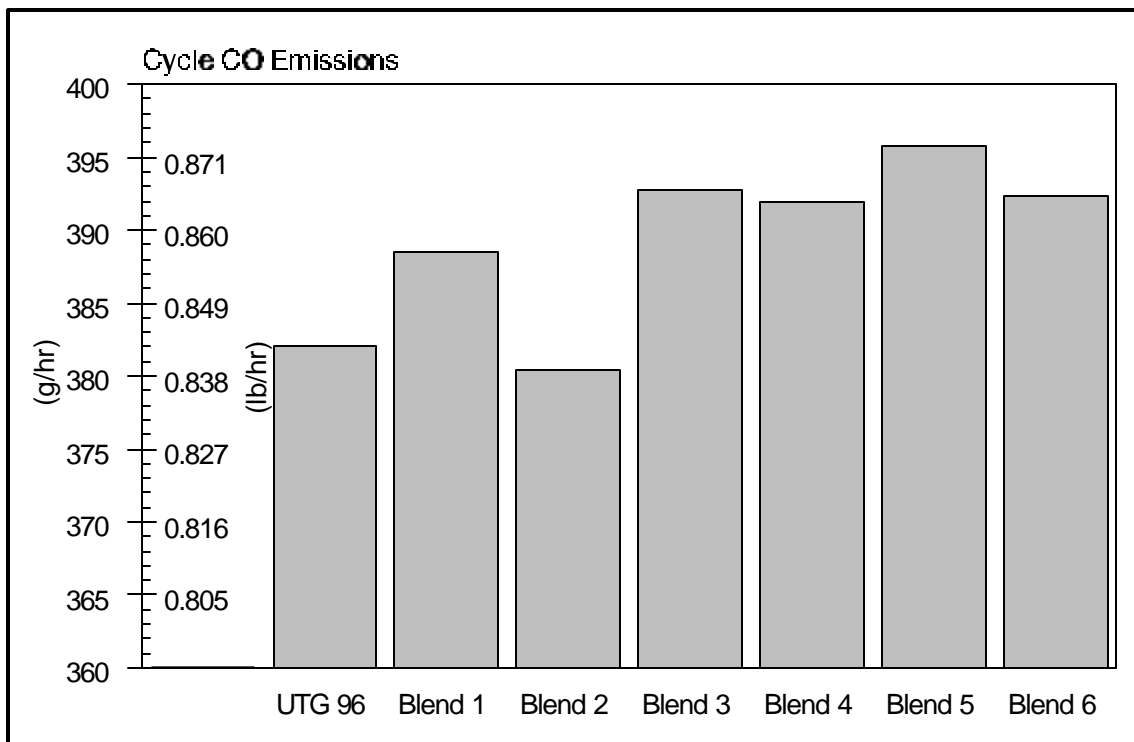


Figure 6 - Cycle CO Emissions

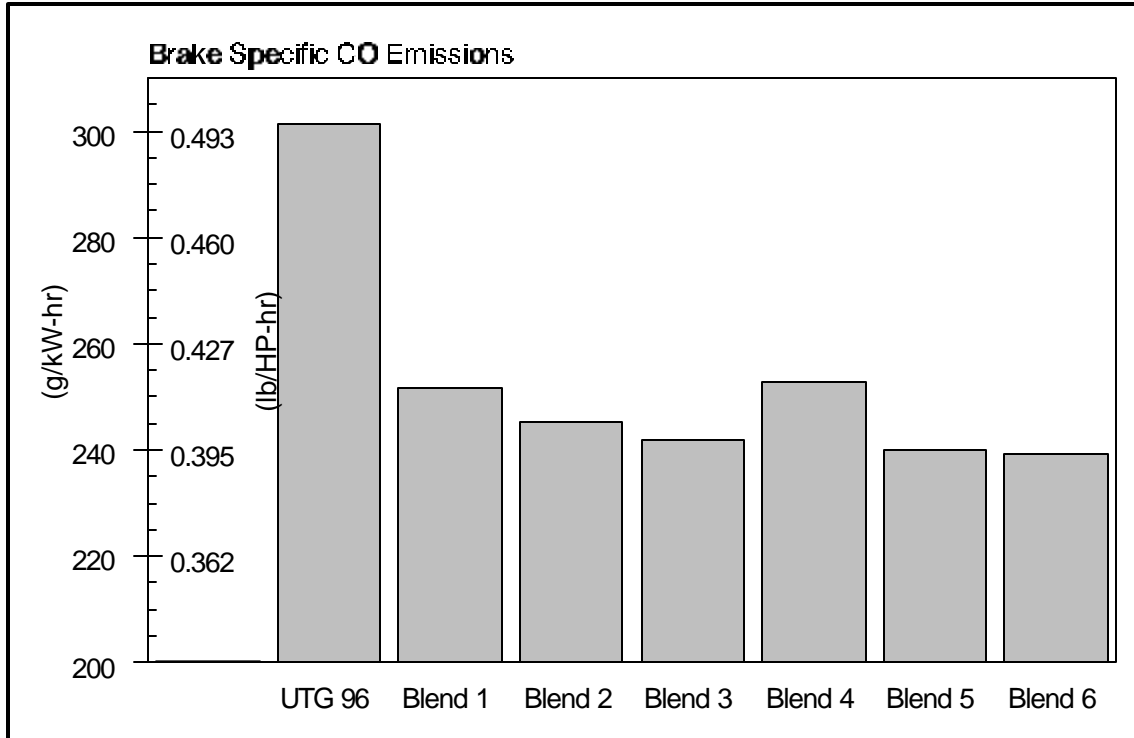


Figure 7 - Brake Specific CO Emissions

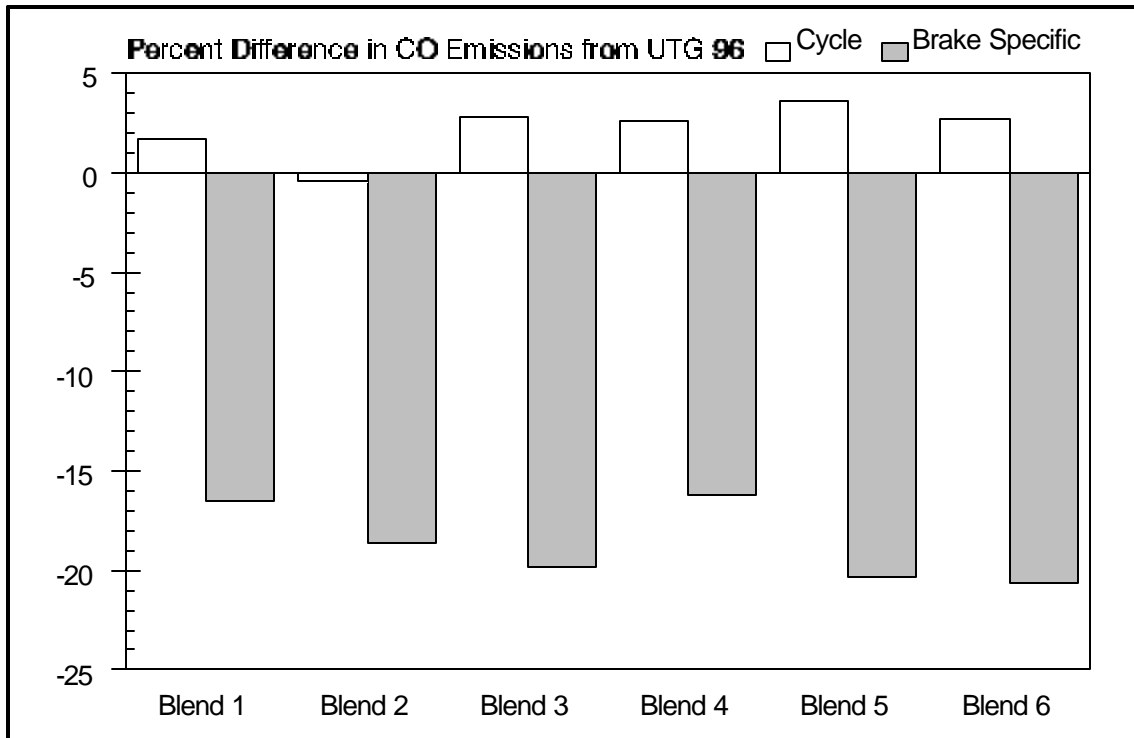


Figure 8 - Percent Difference in CO Emissions Between Blends and UTG 96

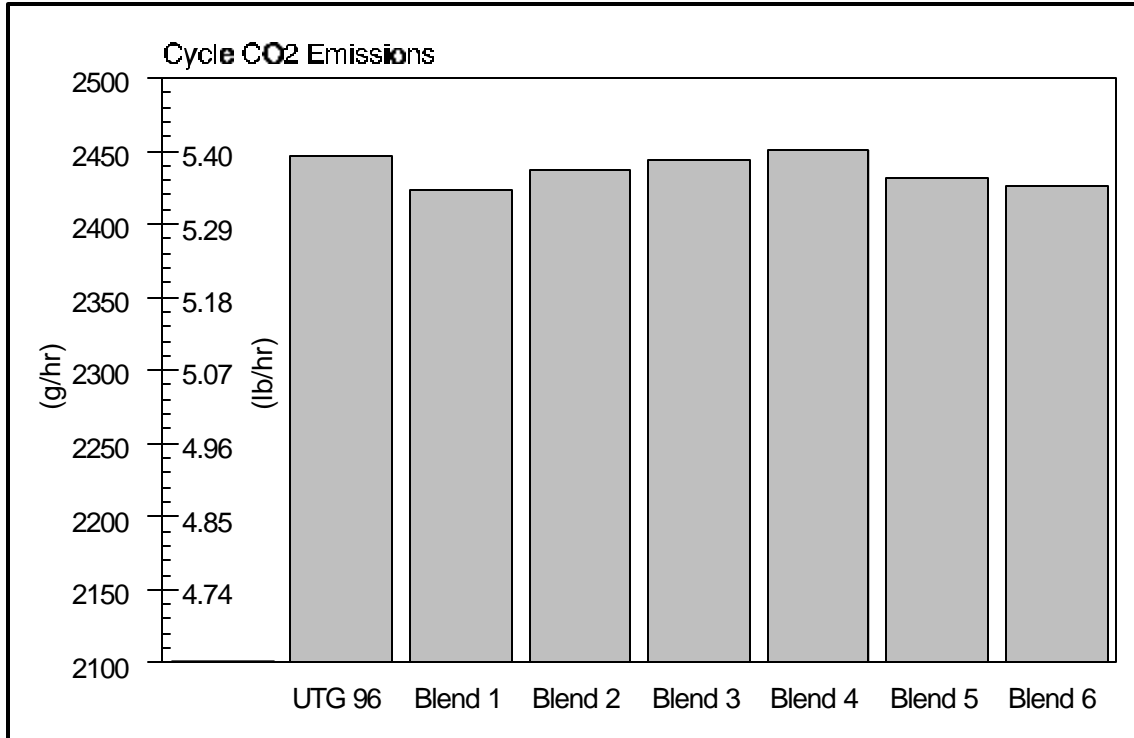


Figure 9 - Cycle CO₂ Emissions

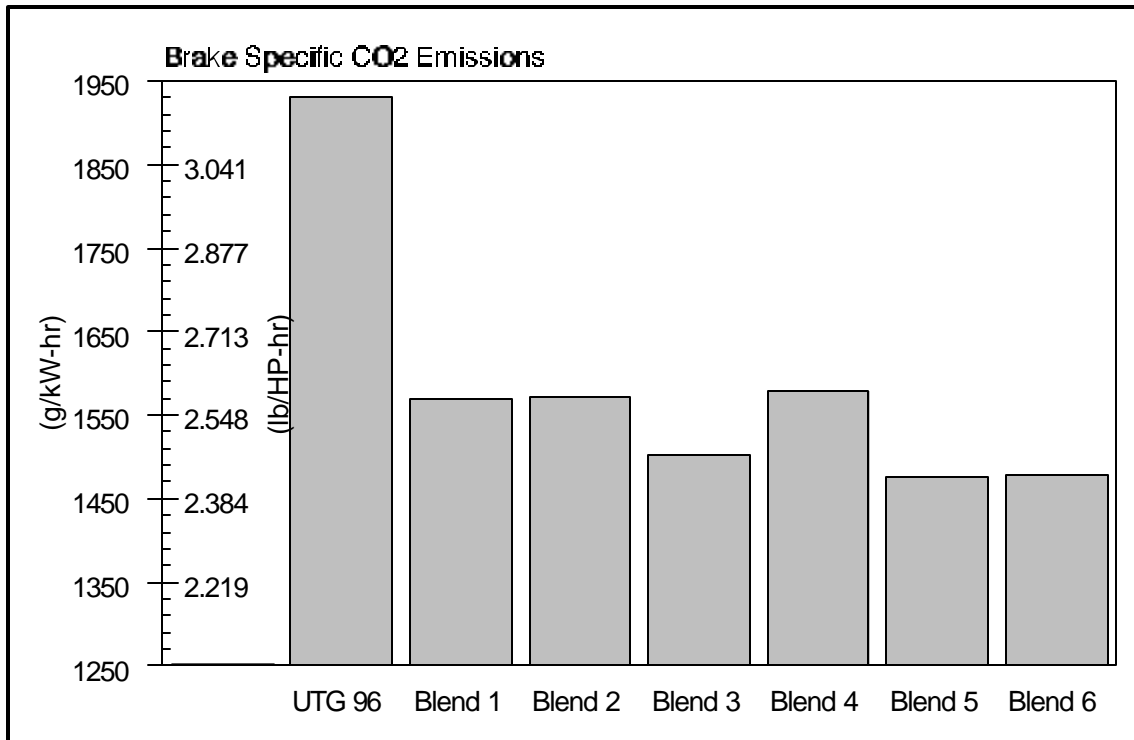


Figure 10 - Brake Specific CO₂ Emissions

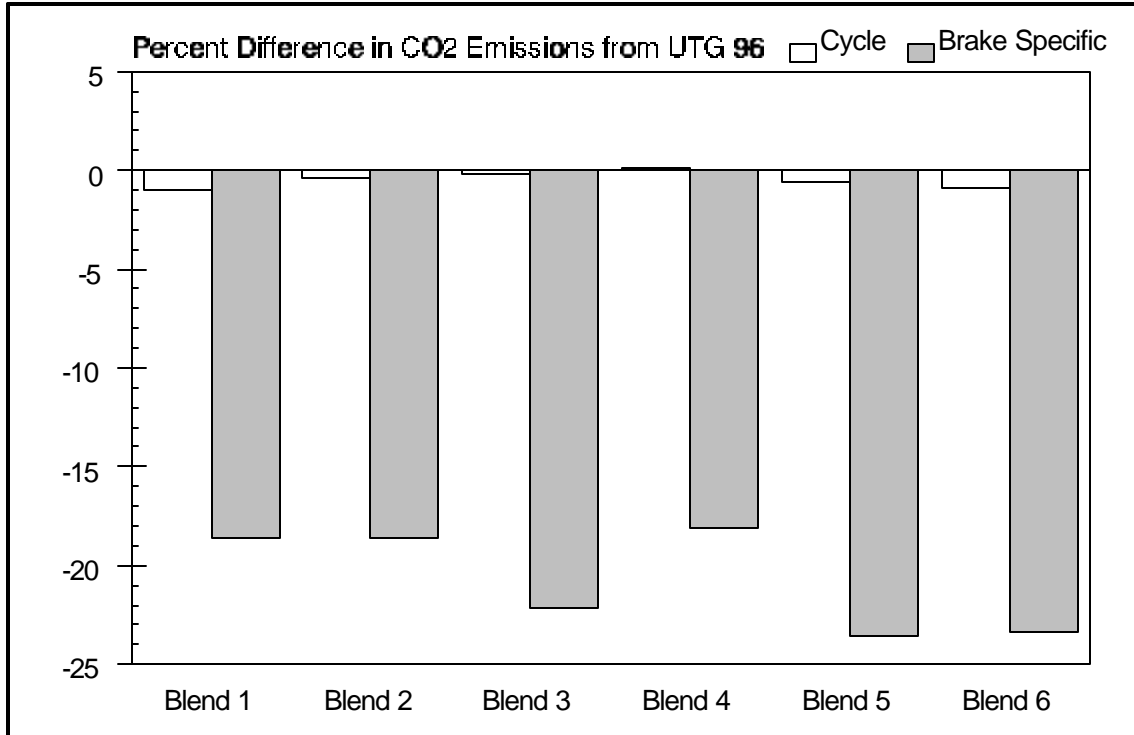


Figure 11 - Percent Difference in CO₂ Emissions Between Blends and UTG 96

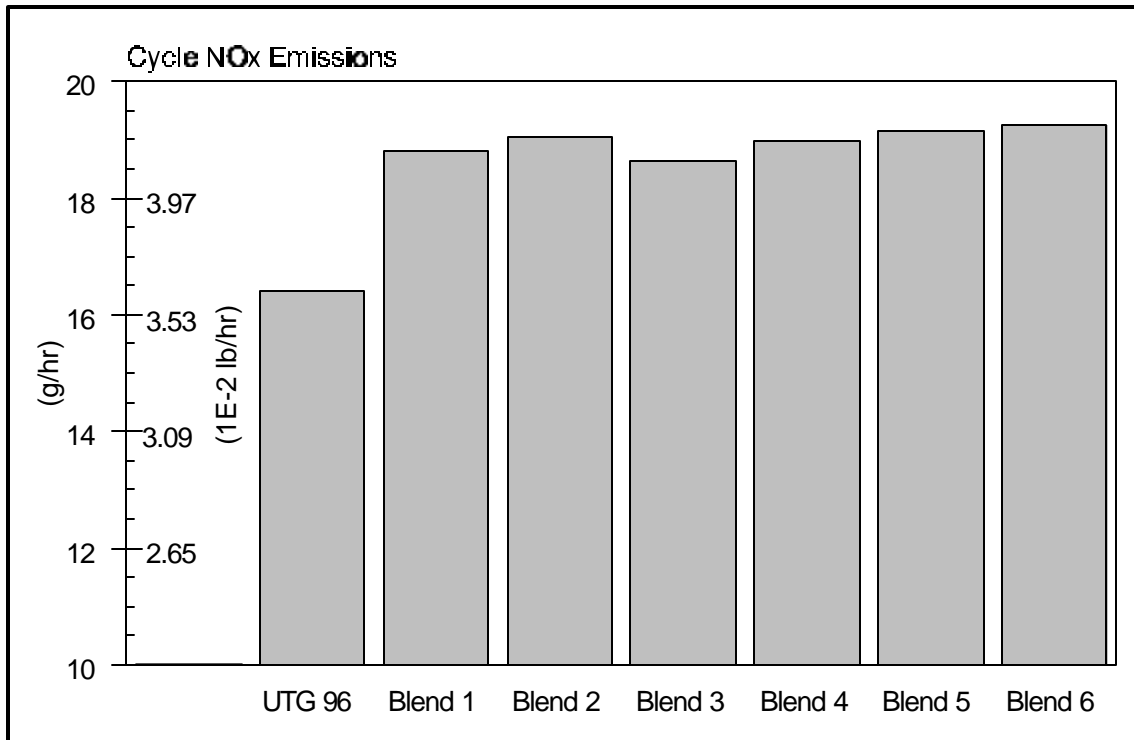


Figure 12 - Cycle NO_x Emissions

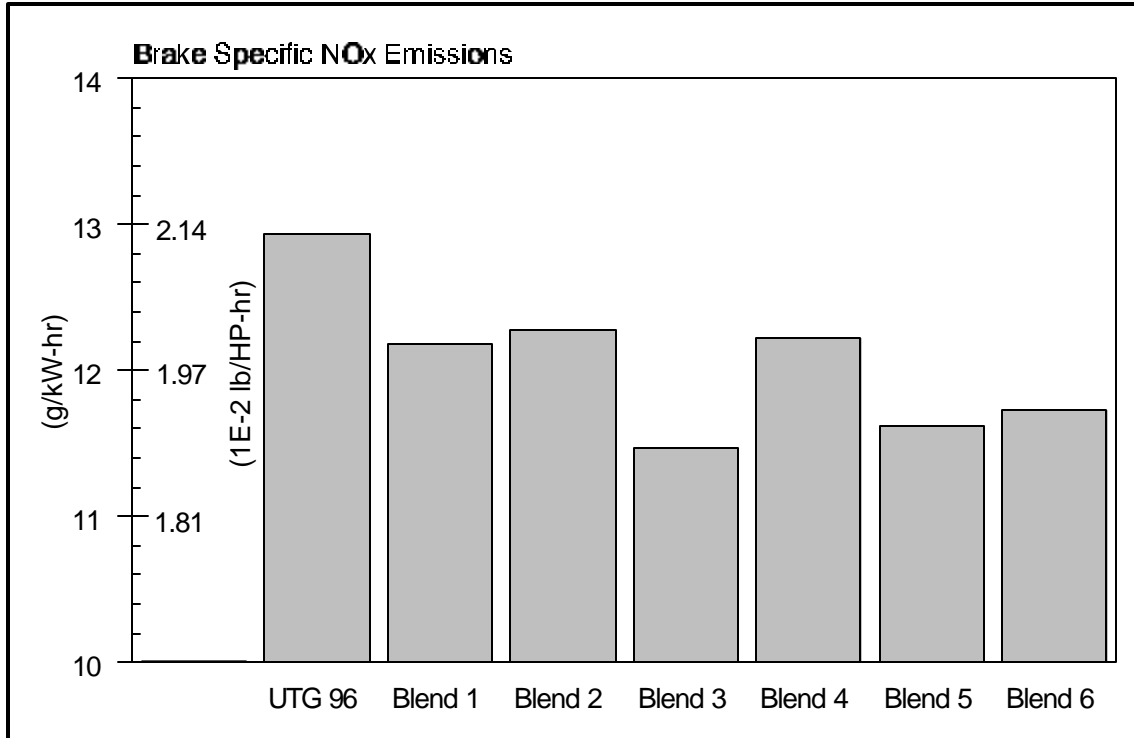


Figure 13 - Brake Specific NO_x Emissions

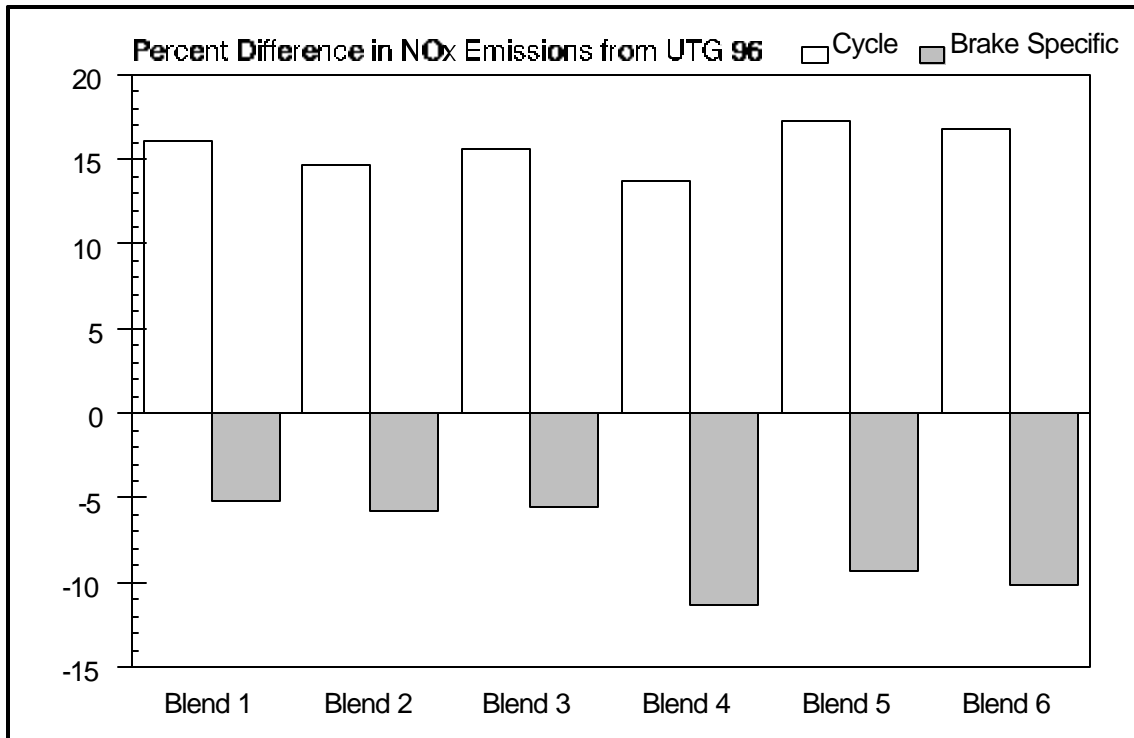


Figure 14 - Percent Difference in NO_x Emissions Between Blends and UTG 96

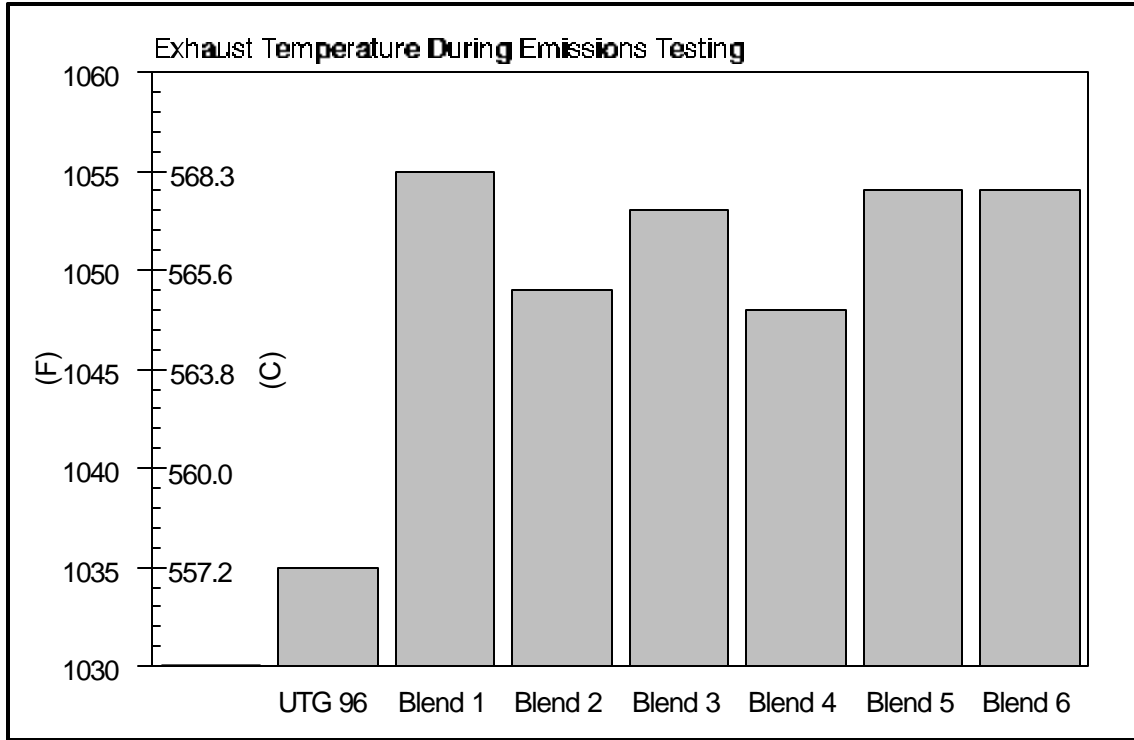


Figure 15 - Exhaust Temperature During Emissions Testing

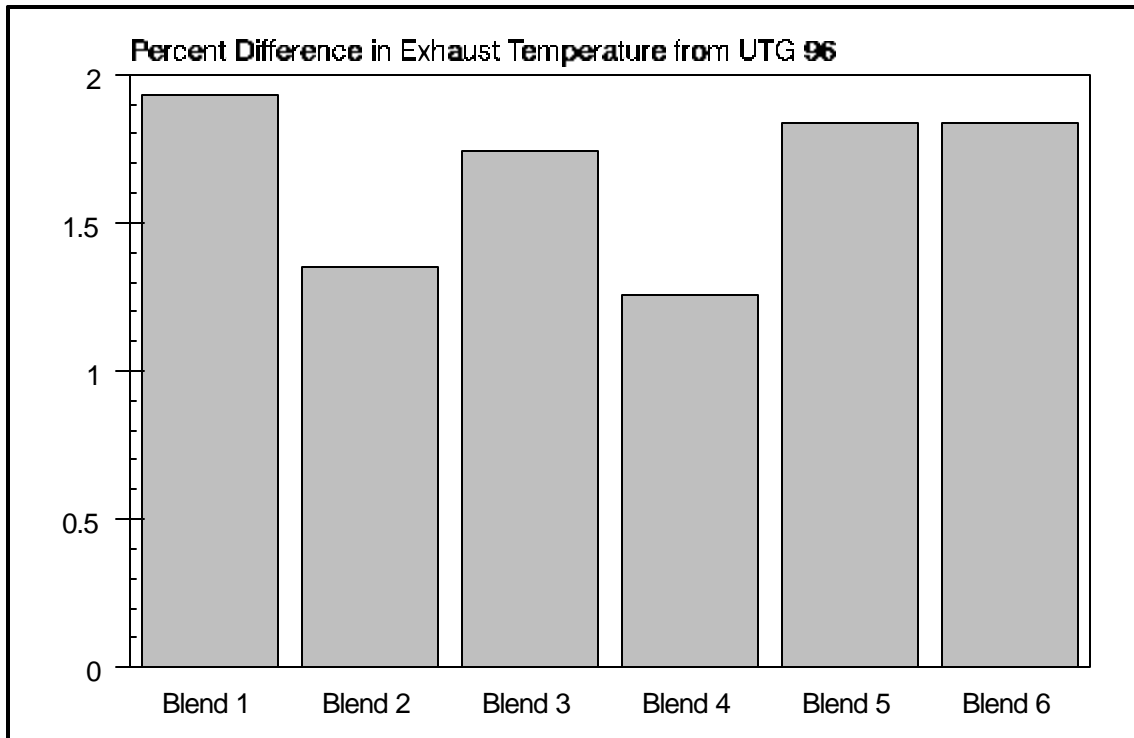


Figure 16 - Percent Difference in Exhaust Temperature Between Blends and UTG 96 During Emissions Testing

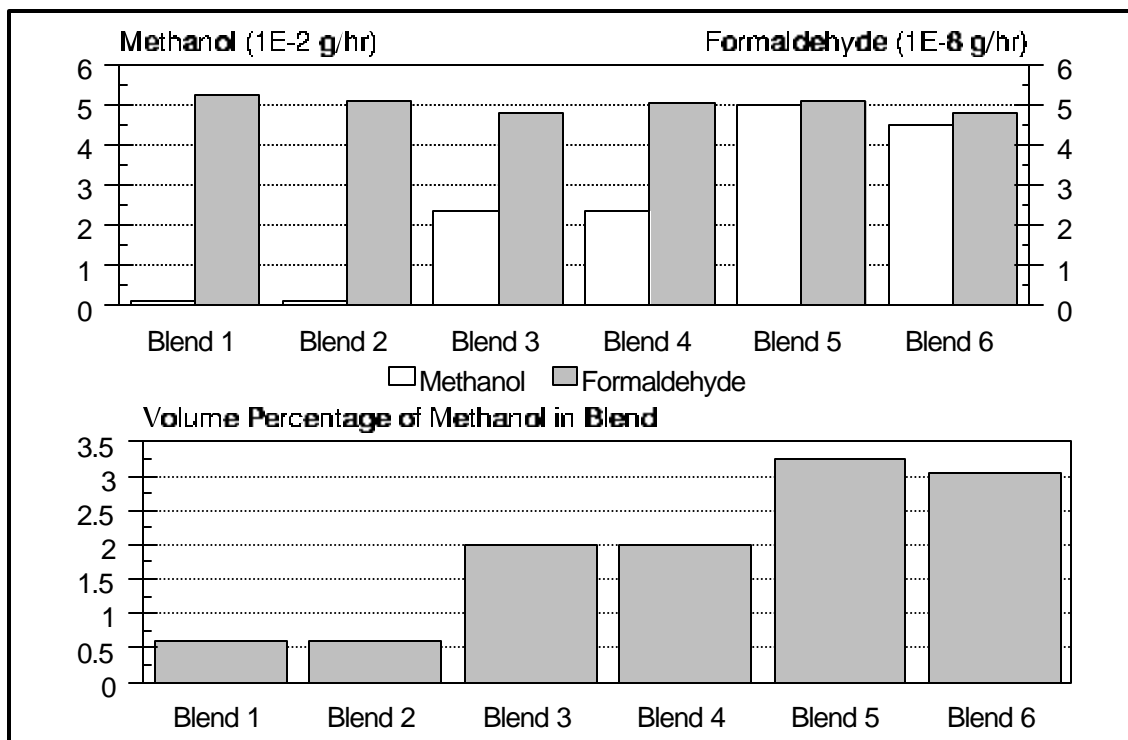


Figure 17 - Methanol and Formaldehyde Emissions and Volume Percentages of Methanol for the Blends

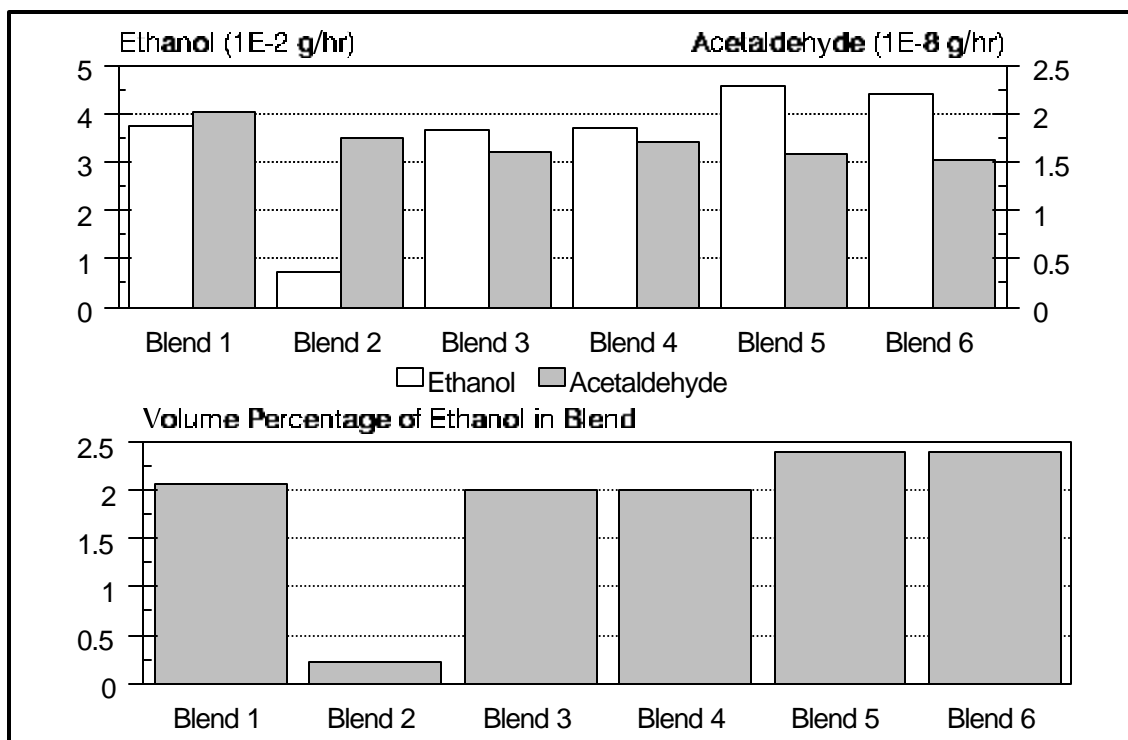


Figure 18 - Ethanol and Acetaldehyde Emissions and Volume Percentages of Ethanol for the Blends

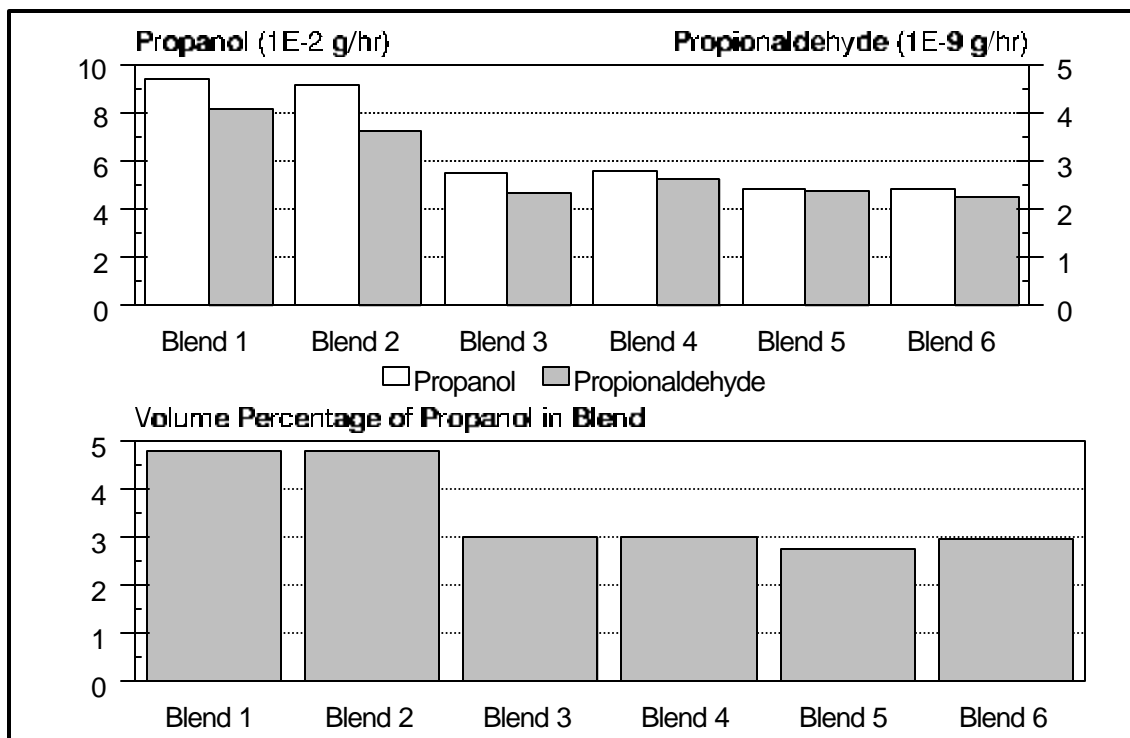


Figure 19 - Propanol and Propionaldehyde Emissions and Volume Percentages of Propanol for the Blends

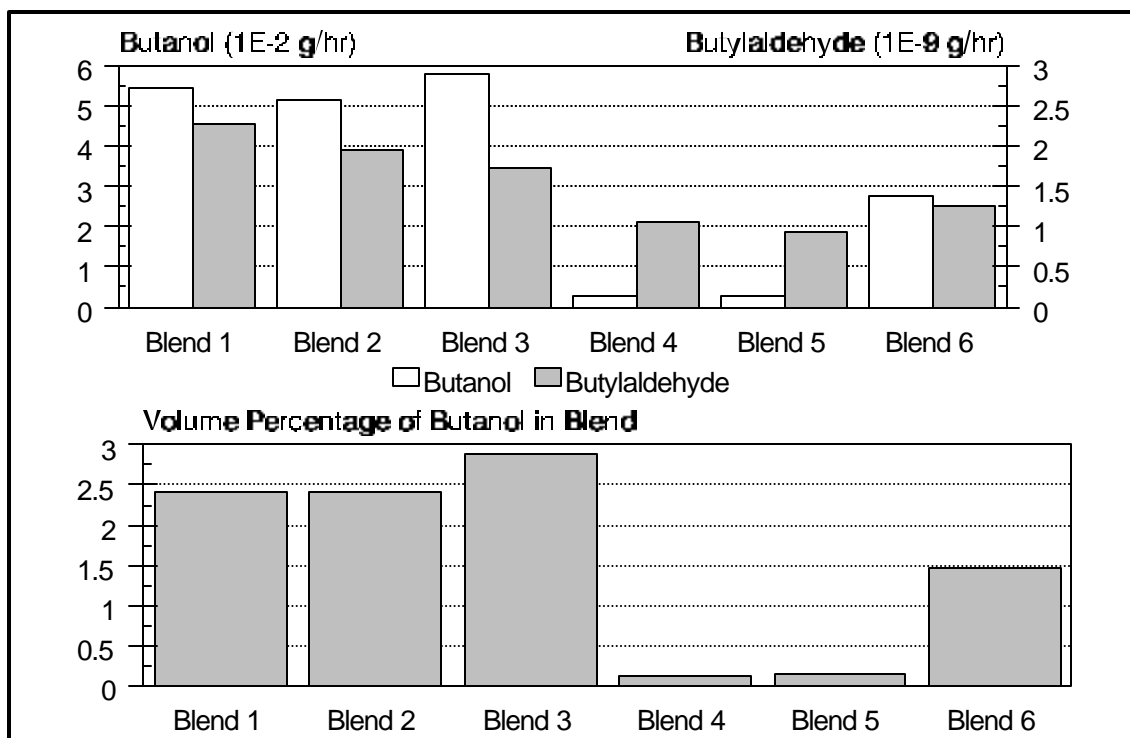


Figure 20 - Butanol and Butylaldehyde Emissions and Volume Percentages of Butanol for the Blends

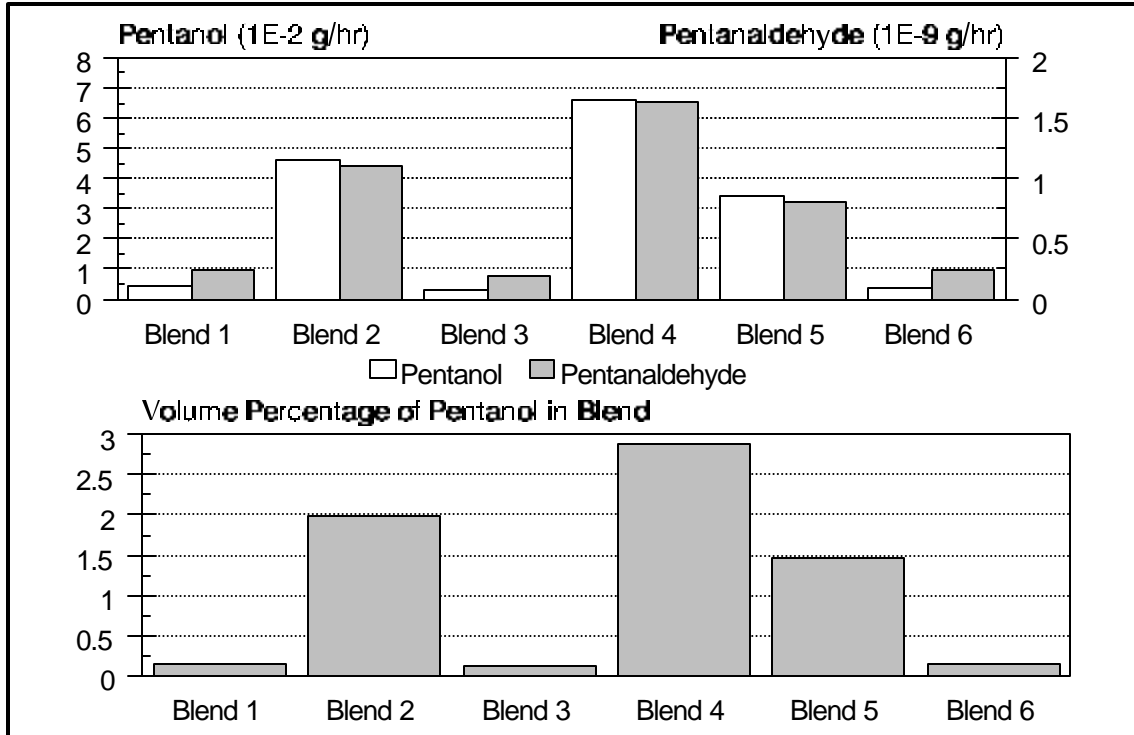


Figure 21 - Pentanol and Pentanaldehyde Emissions and Volume Percentages of Pentanol for the Blends

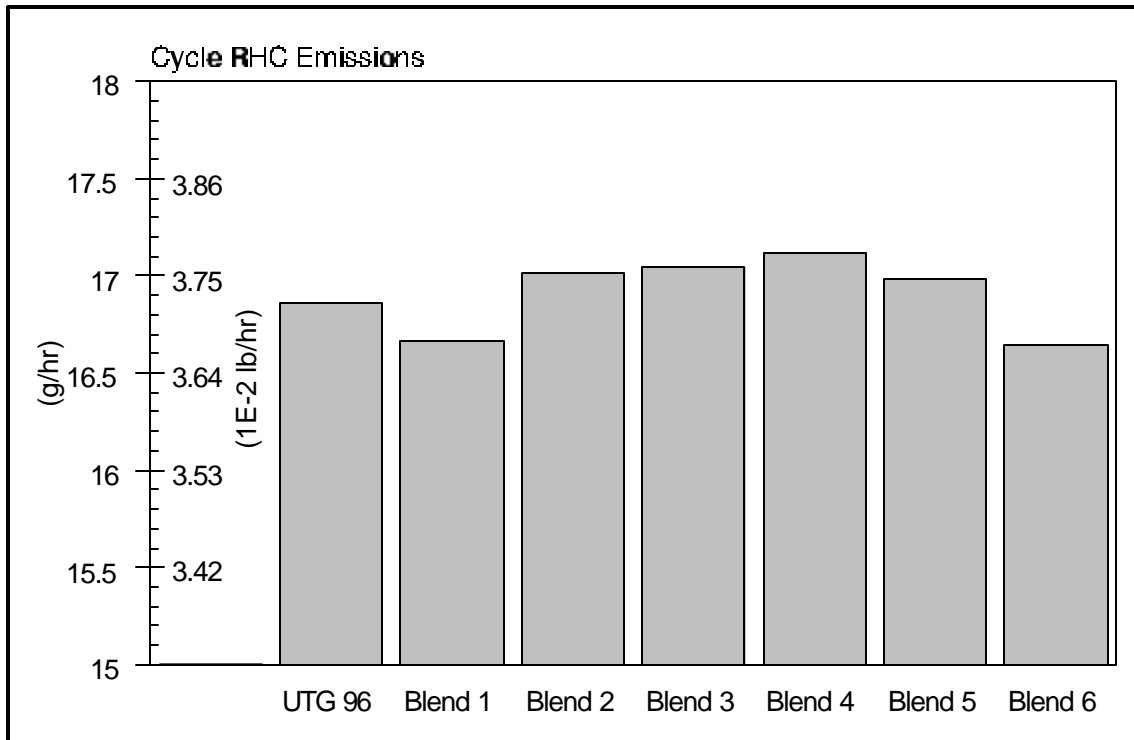


Figure 22 - Cycle RHC Emissions

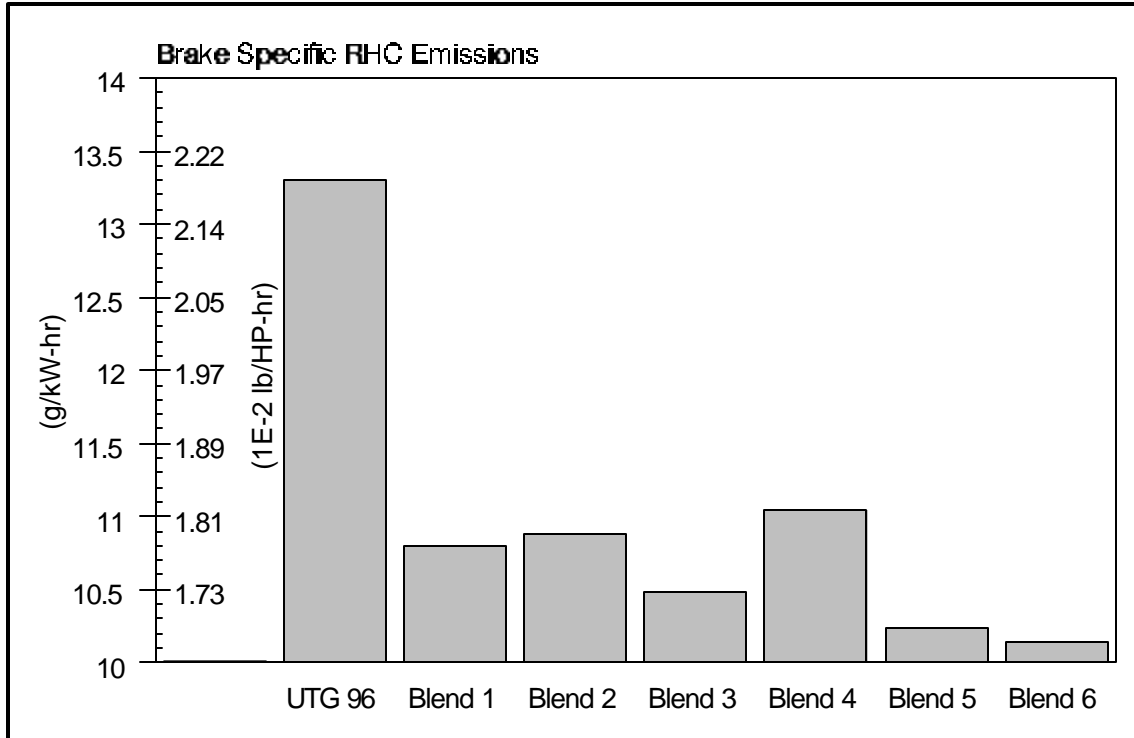


Figure 23 - Brake Specific RHC Emissions

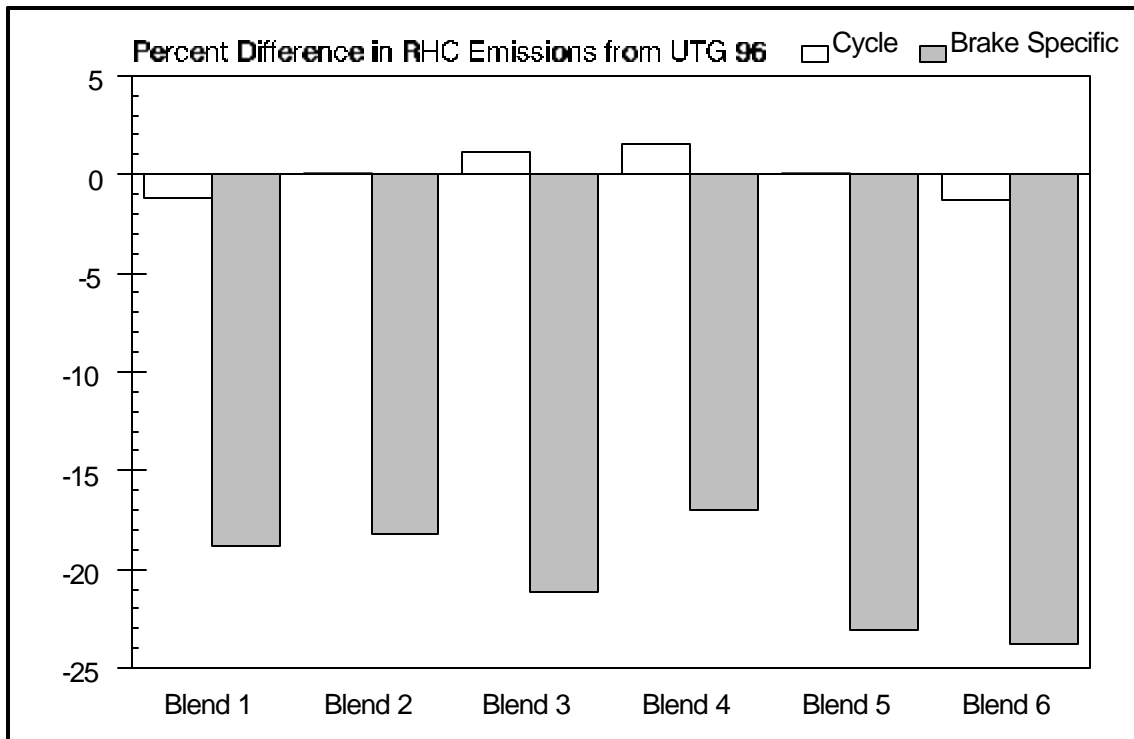


Figure 24 - Percent Difference in RHC Emissions Between Blends and UTG 96

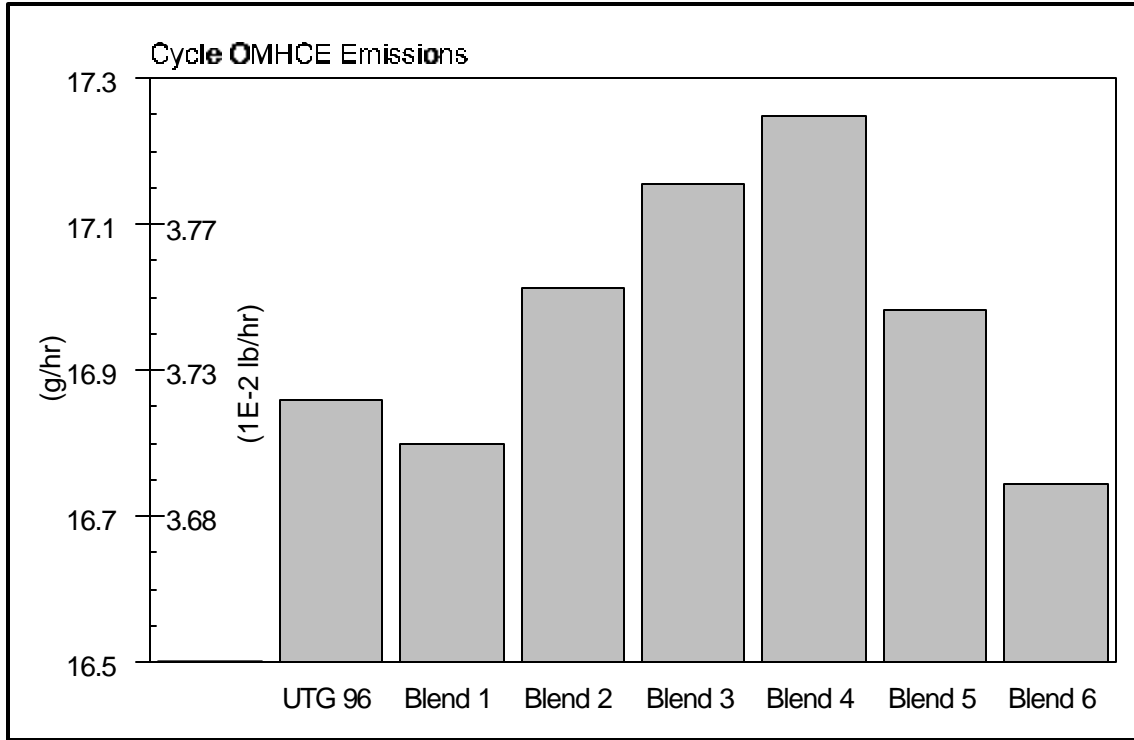


Figure 25 - Cycle OMHCE Emissions

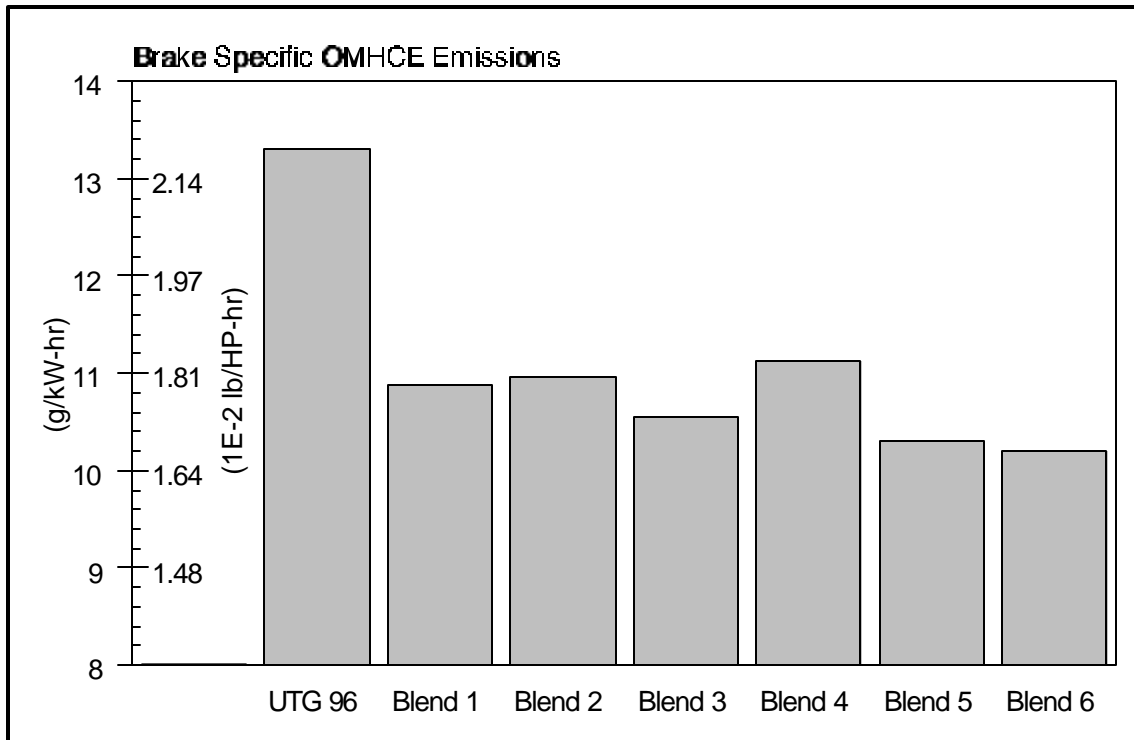


Figure 26 - Brake Specific OMHCE Emissions

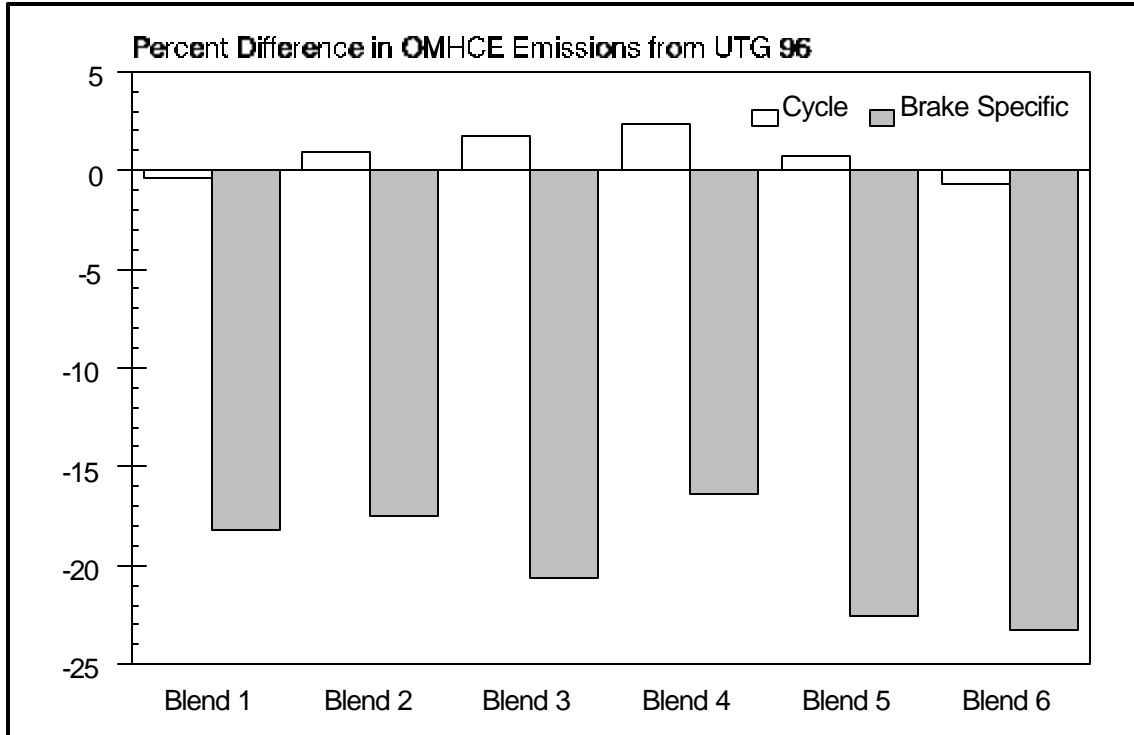


Figure 27 - Percent Difference in OMHCE Emissions Between Blends and UTG 96

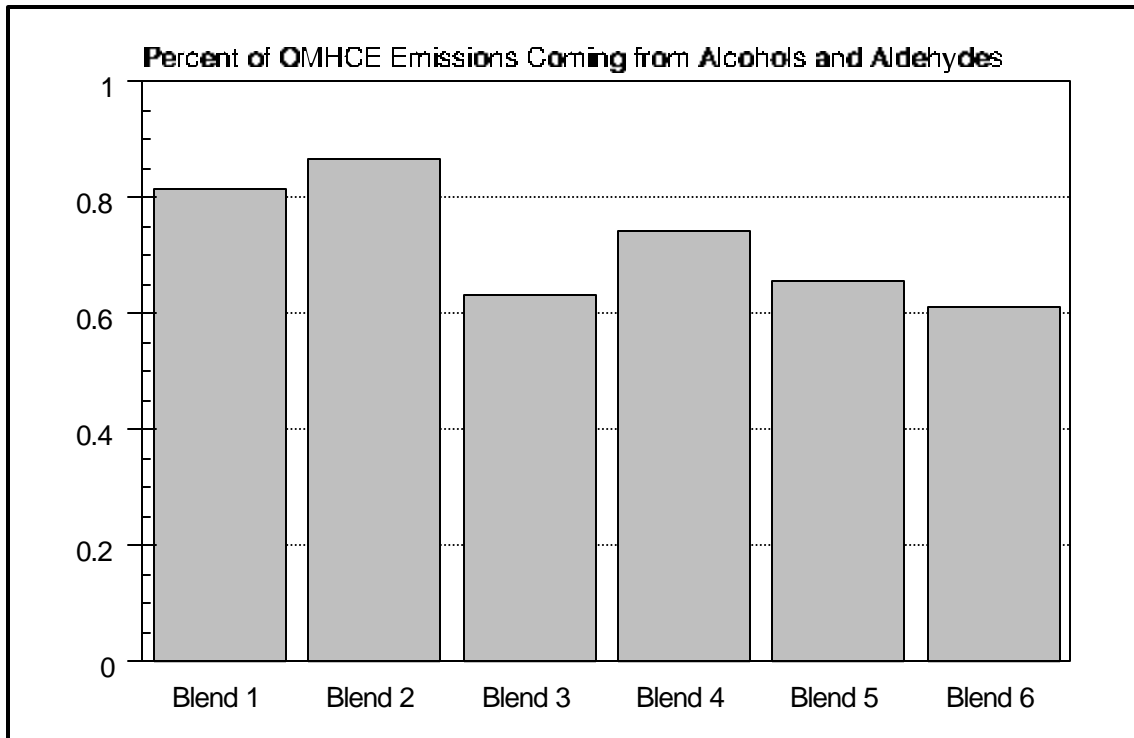


Figure 28 - Percentage of OMHCE Emissions Coming From Alcohols and Aldehydes

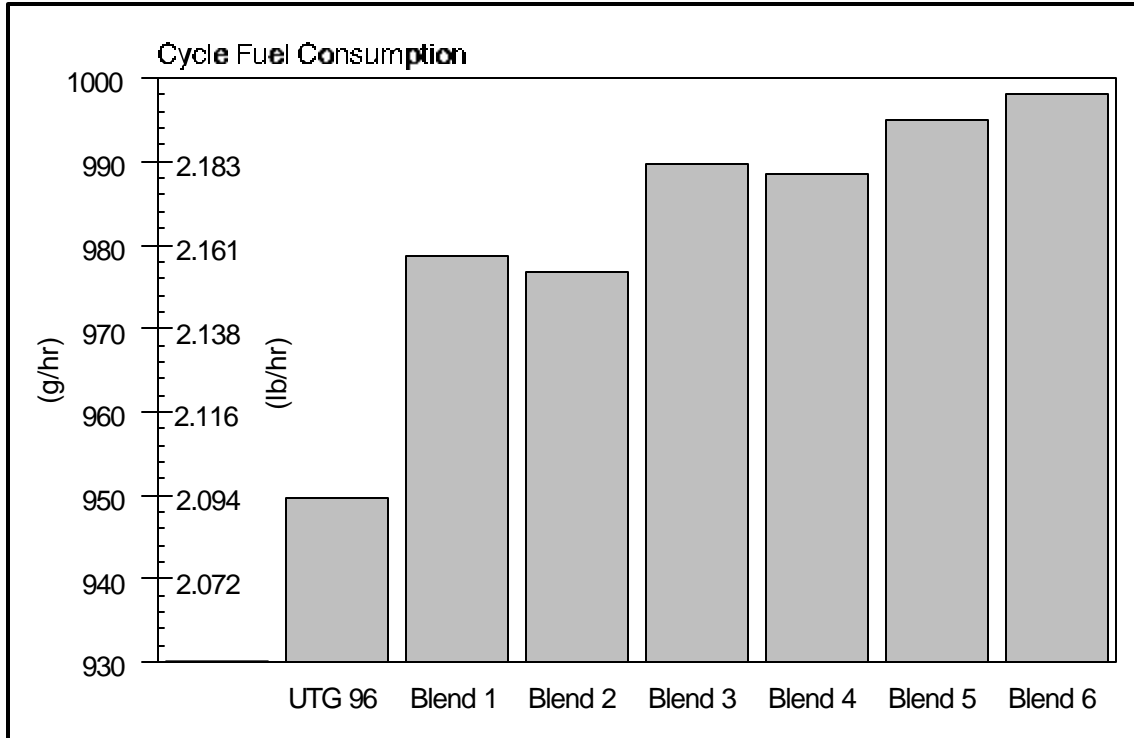


Figure 29 - Cycle Fuel Consumption of the Blends and UTG 96

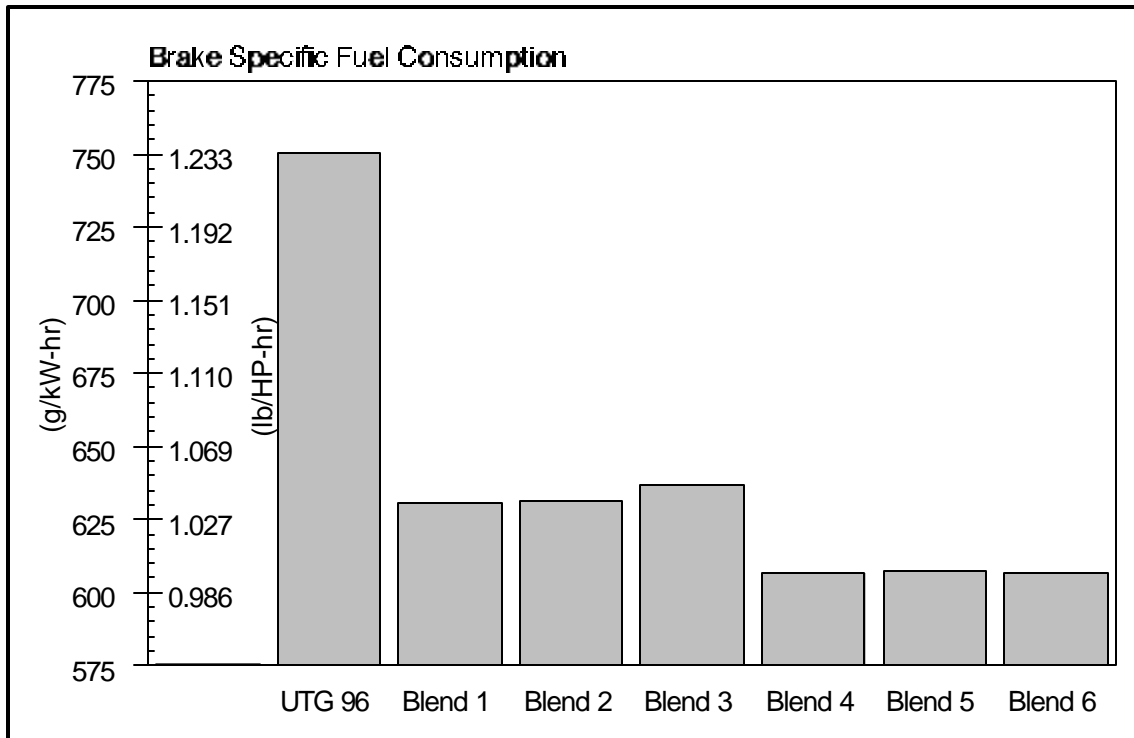


Figure 30 - Brake Specific Fuel Consumption of the Blends and UTG 96

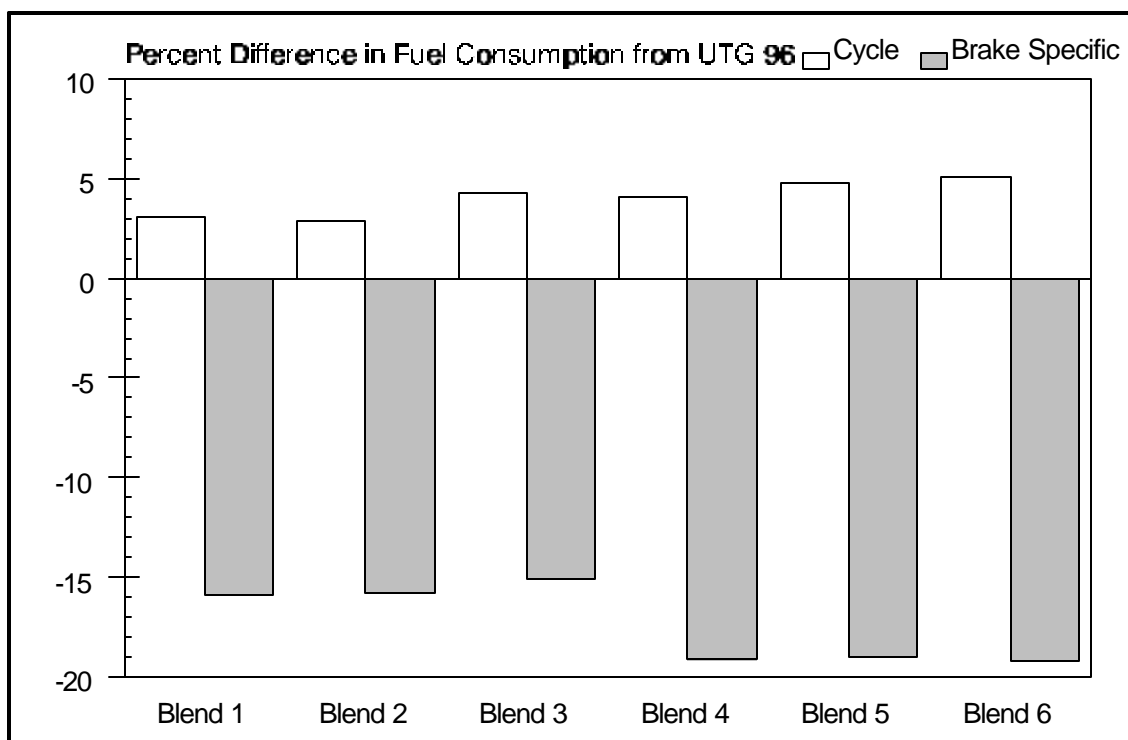


Figure 31 - Percent Difference in Fuel Consumption Between Blends and UTG 96

Reid Vapor Pressure and Distillation

The RVP for each blend and UTG 96 is shown in Figure 32. RVP is a measure of the difficulty in controlling the evaporative emissions from a fuel. The higher the RVP, the more difficult it is to control evaporative emissions and vice versa. Blend 1 (2.67% methanol/ethanol, 7.33% higher alcohols) showed only a slight increase in RVP compared to UTG 96, and blend 2 (0.82% methanol/ethanol, 9.18% higher alcohols) actually showed a small decrease in RVP compared to UTG 96. Blends 5 and 6 had the highest RVP out of all the blends, and these two blends also contained the highest amounts of the lower alcohols (5.64% methanol/ethanol for blend 5 and 5.44% methanol/ethanol for blend 6). Blends 3 and 4 also show the effectiveness of higher order alcohols help in controlling the RVP of the blend. It should be noted that blend 4 had an RVP lower than blend 3. The compositions of blends 3 and 4 were identical except that blend 3 contained 2.88% butanol and 0.12% pentanol, whereas blend 4 contained 0.12% butanol and 2.88% pentanol. Blends 5 and 6 illustrate how high order alcohols can offset the effects of lower alcohols on RVP. Blend 5 contained 3.24% methanol compared to 3.04% methanol in blend 6. However, these two blends have nearly identical RVPs. The fact that blend 5 contained 1.47% pentanol compared to 0.13% pentanol in blend 6 seemed to offset the higher concentration of methanol in blend 5.

It has been shown by previous researchers that the presence of alcohols in gasoline depress the distillation curve of the fuel, which can cause problems with cold starting and vapor lock. This expected trend was true of all the six test blends. Figures 34 - 39 show the distillation curves of the blends and of UTG 96. The distillation curve for each blend was depressed between 0% and 60% points. To determine the effects of the different alcohols on the distillation curve, the area under each curve between 0% and 60% evaporated was numerically calculated

(see Figure 40). Blends 1 and 2 showed the least effects on the distillation curve from the alcohols, but it should be noted that these blends also contain the least methanol/ethanol. Blend 2 shows a lower effect on distillation than blend 1, and, as mentioned previously, blend 2 had lower methanol/ethanol concentration than blend 1. Blends 5 and 6 showed the greatest effect on the distillation curve, and these blends contained the highest amounts of methanol/ethanol. Thus, it becomes obvious that the lower alcohols have a more significant effect on the distillation curve than the higher alcohols.

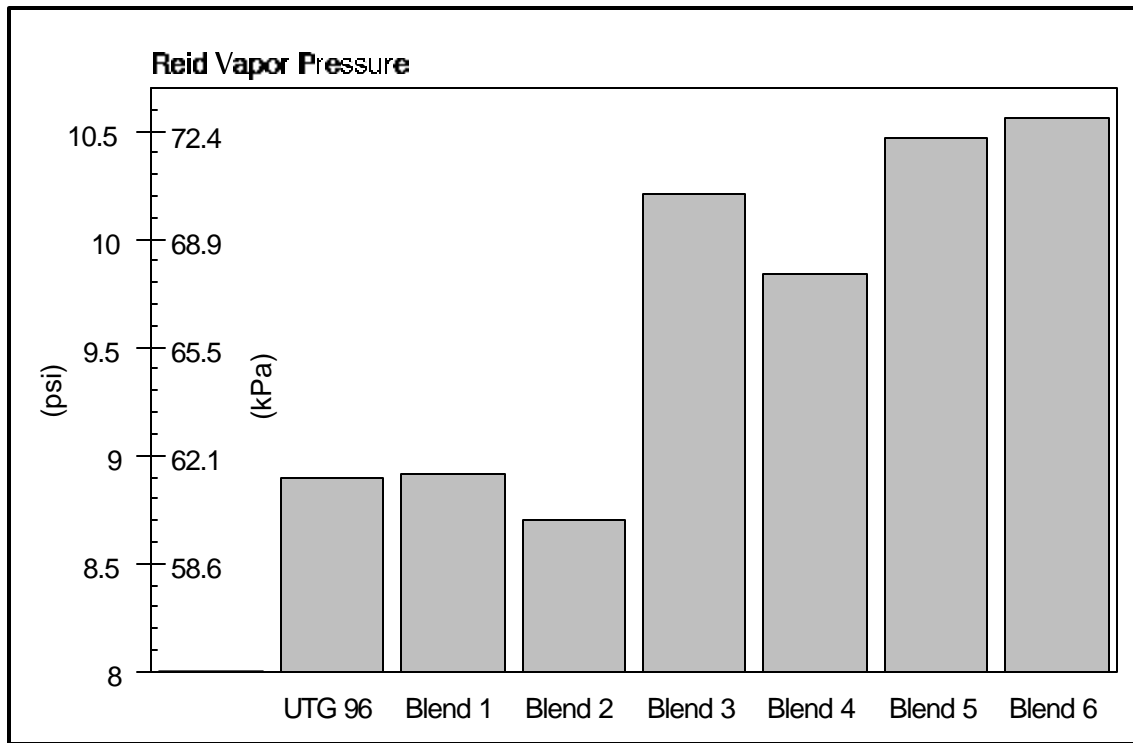


Figure 32 - Reid Vapor Pressures of the Blends and UTG 96

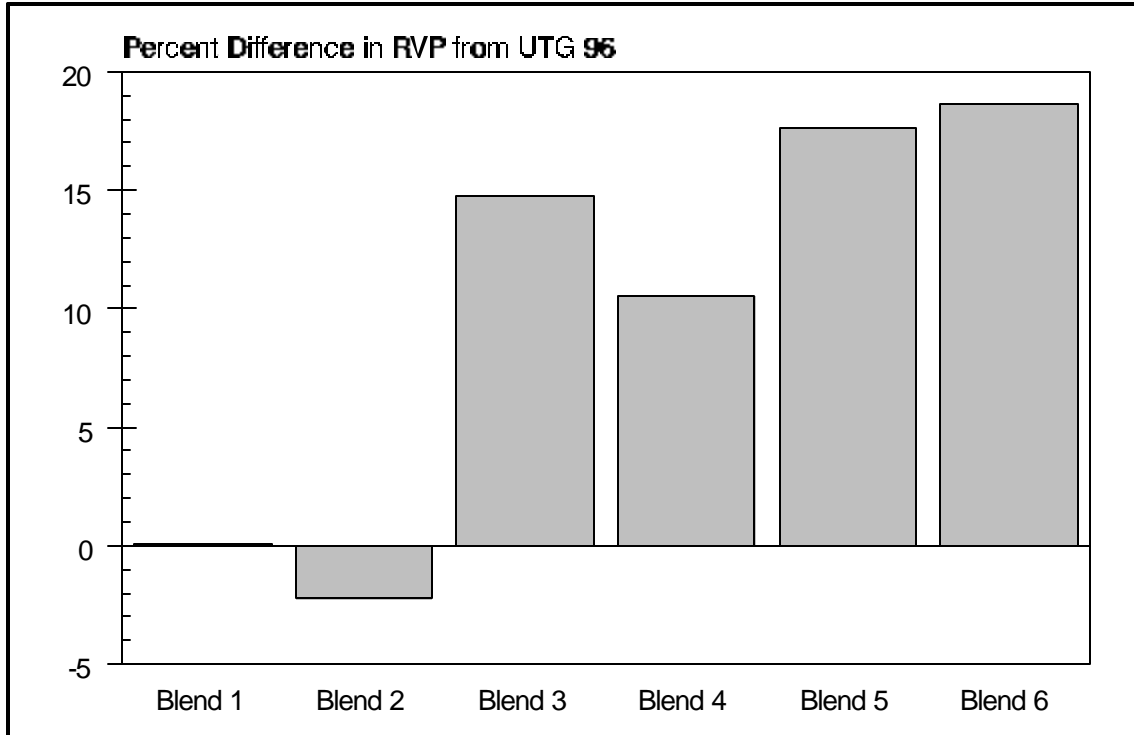


Figure 33 - Percent Difference in RVP Between Blends and UTG 96

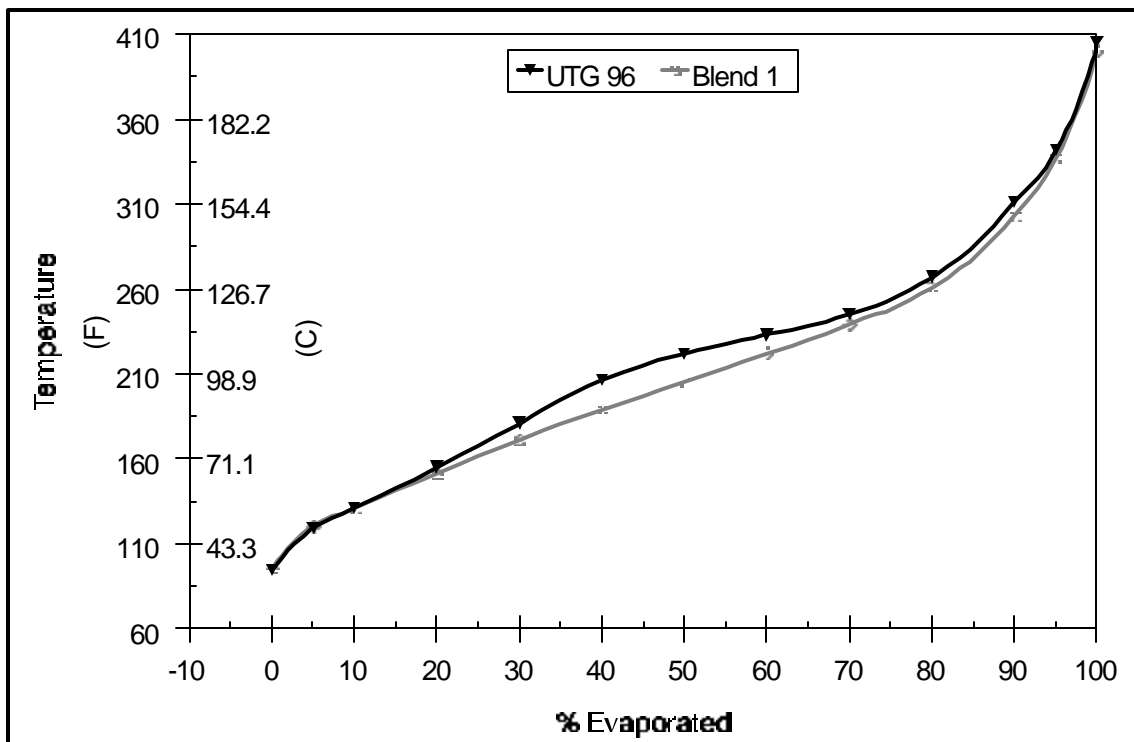


Figure 34 - Comparison of Distillation Curves Between Blend 1 and UTG 96

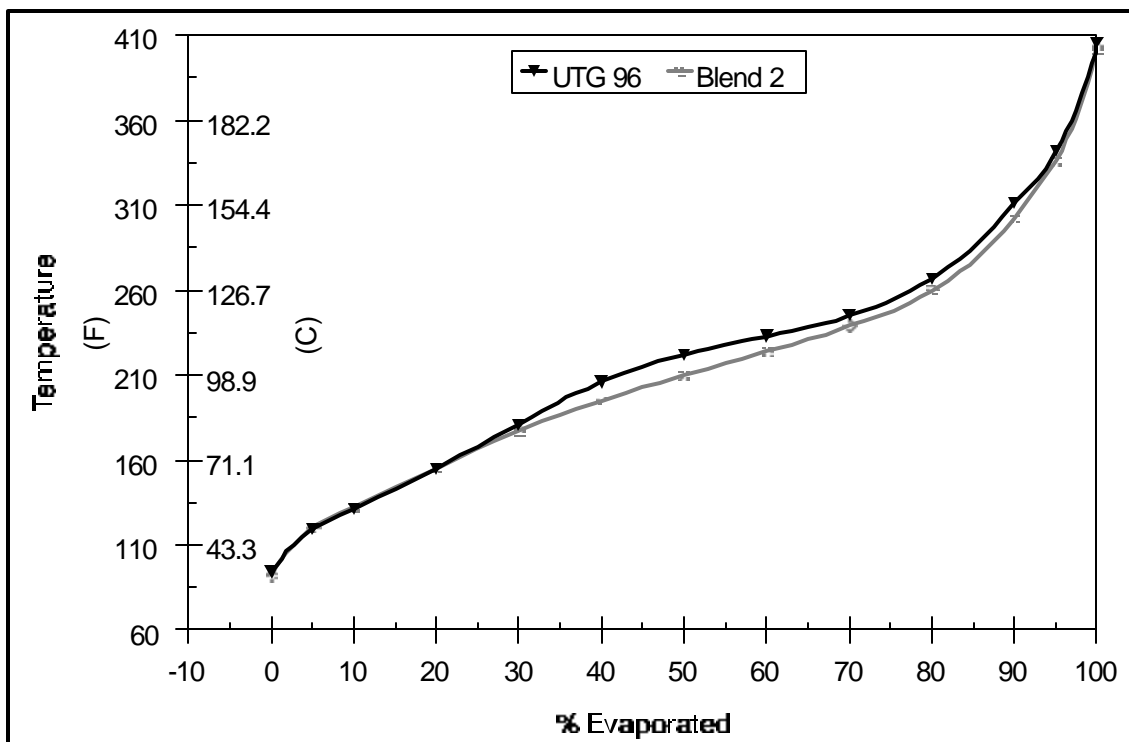


Figure 35 - Comparison of Distillation Curves Between Blend 2 and UTG 96

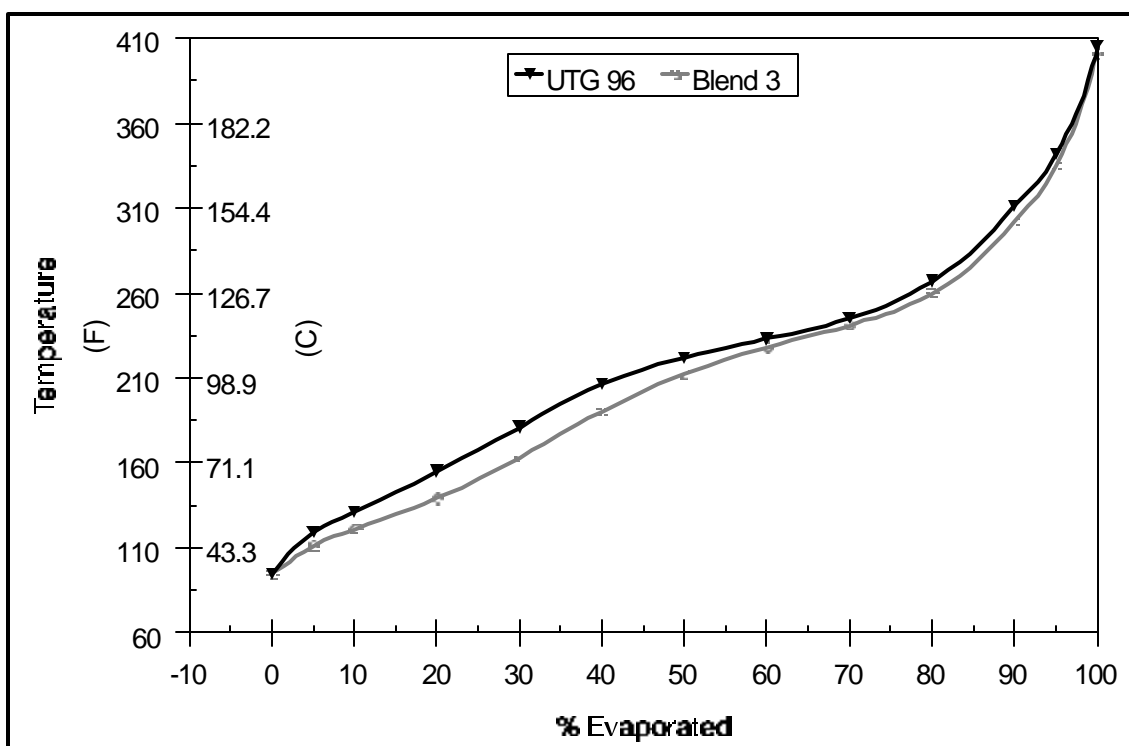


Figure 36 - Comparison of Distillation Curves Between Blend 3 and UTG 96

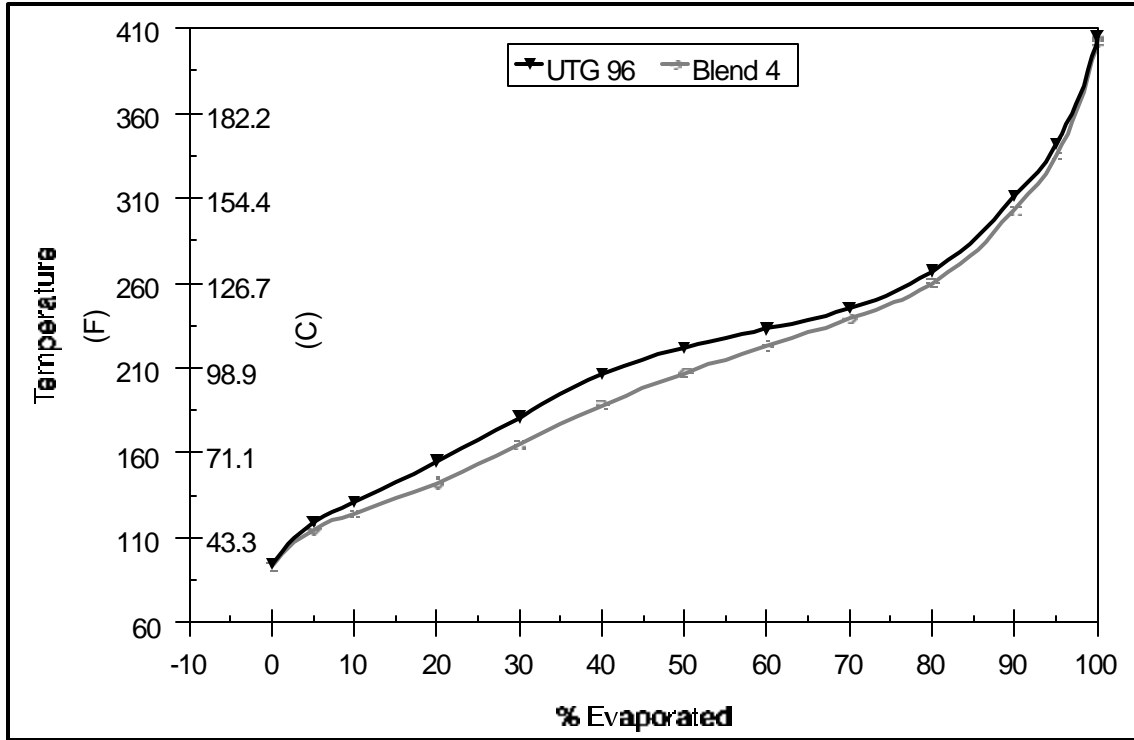


Figure 37 - Comparison of Distillation Curves Between Blend 4 and UTG 96

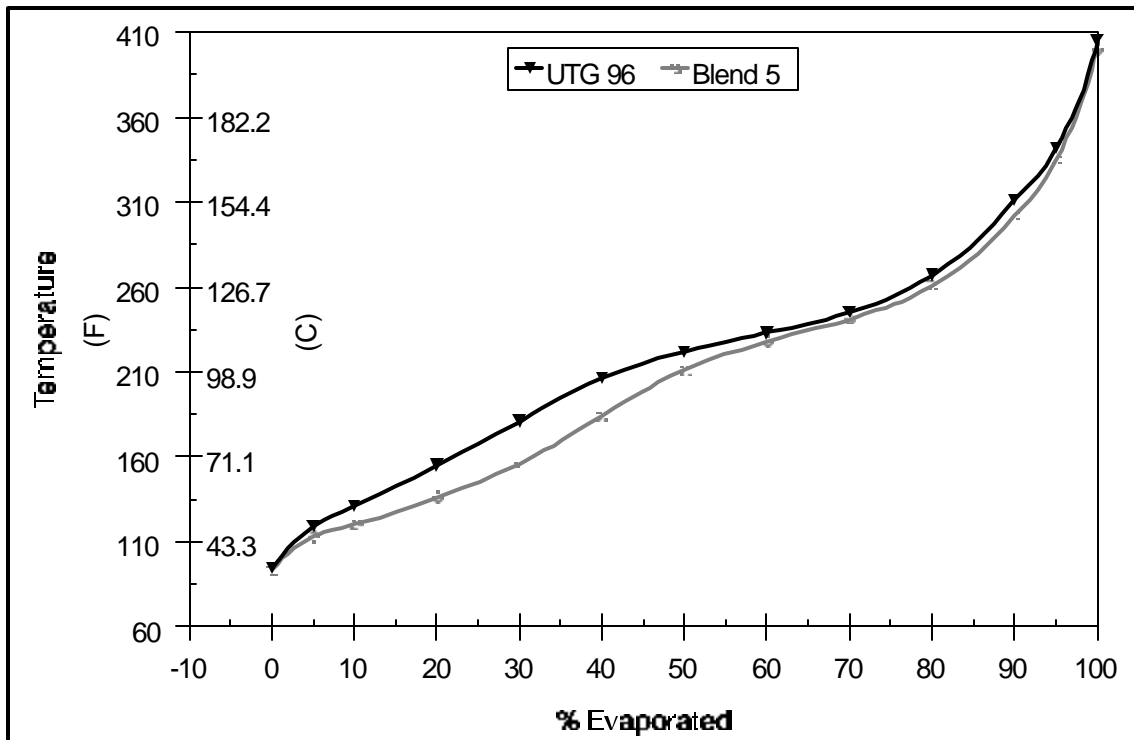


Figure 38 - Comparison of Distillation Curves Between Blend 5 and UTG 96

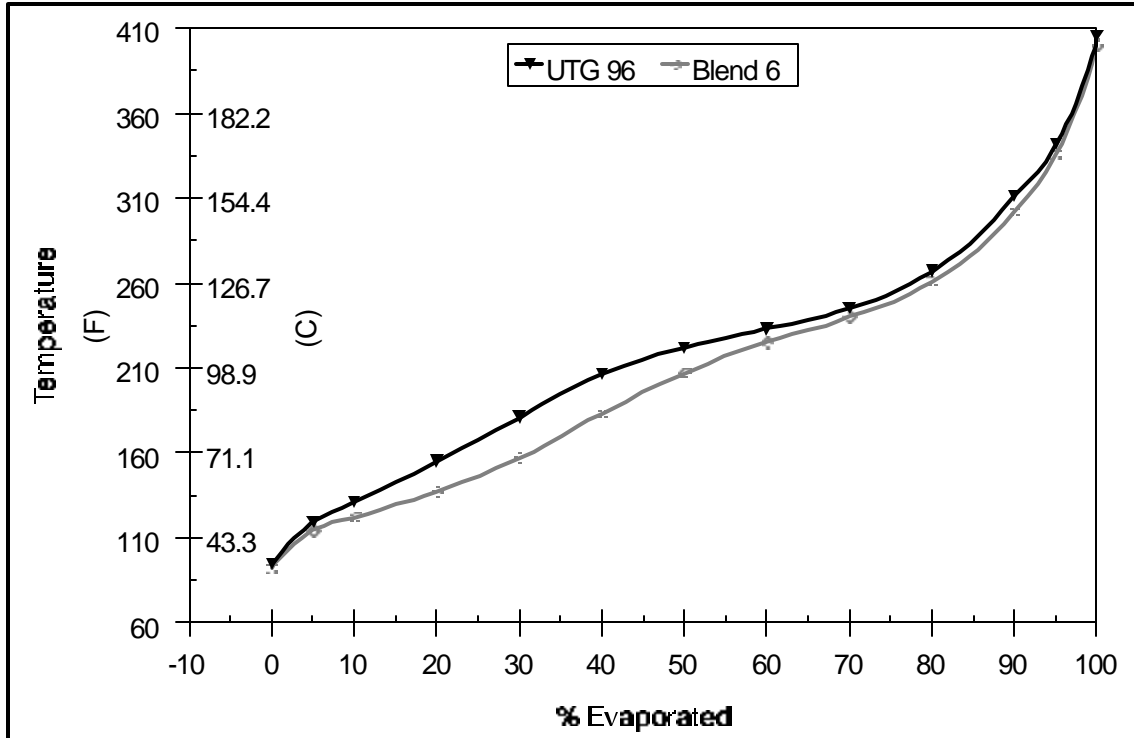


Figure 39 - Comparison of Distillation Curves Between Blend 6 and UTG 96

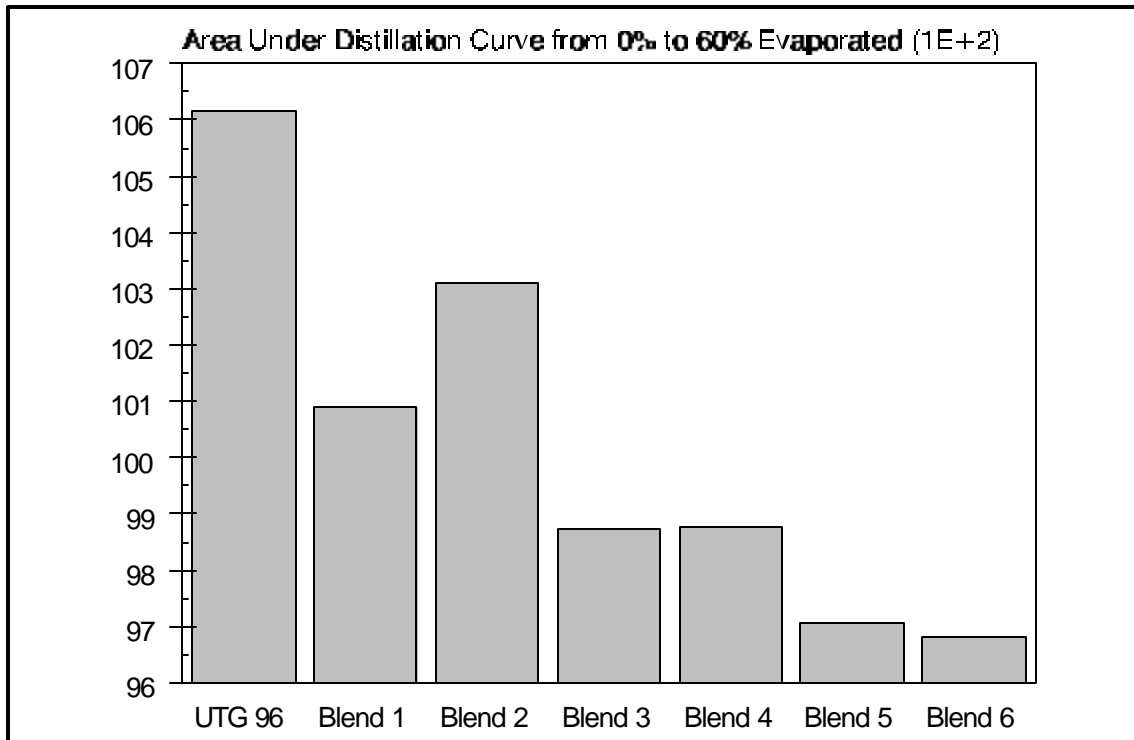


Figure 40 - Comparison of the Area Under the Distillation Curve Between 0% and 60% Evaporated for the Blends and UTG 96

Conclusions

An experimental investigation of emissions characteristics of higher alcohols/gasoline (UTG 96) blends was conducted. In order to carry out the experiments, a single cylinder engine was instrumented and the necessary data acquisition and data reduction computer programs were written. Comparisons of emissions and fuel characteristics between higher alcohol/gasoline blends and neat gasoline were made to determine the advantages and disadvantages of blending alcohol with gasoline. All tests were conducted on a single cylinder Waukesha CFR engine at steady state conditions and stoichiometric A/F ratio.

Emissions tests were conducted at the optimum spark timing-KLCR combination (i.e. the point of maximum power) for the particular blend being tested. The cycle emissions (mass per unit time) of CO, CO₂, and organic matter hydrocarbon equivalent (OMHCE) from the higher alcohol/gasoline blends are all within 5% of those emissions from neat gasoline. Cycle emissions of NO_x from the blends were 15% - 18% higher than those from neat gasoline. However, for all the emissions species considered, the brake specific emissions (mass per unit time per unit power output) were significantly lower for the higher alcohol/gasoline blends than for neat gasoline (16% - 20% lower CO, 18% - 23% lower CO₂, 5% - 11% lower NO_x, and 17% - 23% lower OMHCE). This is due to the fact that the blends had greater resistance to knock and allowed higher compression ratios, which increased engine power output. Thus, the brake specific emissions were lower. The contribution of alcohols and aldehydes to the overall OMHCE emissions was found to be less than 1% for every blend tested and, thus, made up a minimal amount of the total hydrocarbon emissions.

Cycle fuel consumption (mass per unit time) of higher alcohol/gasoline blends ranged from 3% to 5% higher than neat gasoline due to the lower stoichiometric A/F ratios required by the blends. However, the brake specific fuel consumption (BSFC) (mass per unit time per unit power output) for the blends ranged from 15% - 19% lower than the BSFC of neat gasoline.

The other fuel parameters, RVP and distillation curve, were affected by the addition of alcohol to gasoline. The lower alcohols (methanol and ethanol) cause the most dramatic increase in RVP and the largest depression of the distillation curve. Addition of the higher alcohols (propanol, butanol, and pentanol) seems to curb the effects of methanol and ethanol on RVP and distillation.

References

- American Petroleum Institute, "Alcohols and Ethers, A Technical Assessment of Their Application as Fuels and Fuel Components," API Publication N. 4261, Second Edition, July 1988.
- Bardon, M. F., Gardiner, D. P., and Rao, V. K., "Cold Starting Performance of Gasoline/Methanol M10 Blends in a Spark Ignition Engine," SAE Paper No. 852014, 1985.
- Bata, Reda M., Elrod, Alvon C., and Lewandowski, Thomas P., "Butanol as a Blending Agent with Gasoline for I.C. Engines," SAE Paper No. 890434, 1989.
- Code of Federal Regulations, Protection of the Environment, 40 CFR, Parts 86 to 99, Revised as of July 1, 1994, United States Government Printing Office, Washington D.C., 1994.
- Coordinating Research Council, Inc., "Performance Evaluation of Alcohol-Gasoline Blends in 1980 Model Automobiles - Phase I - Ethanol-Gasoline Blends," CRC Report No. 527, July 1982.
- Coordinating Research Council, Inc., "Performance Evaluation of Alcohol-Gasoline Blends in 1980 Model Automobiles - Phase II - Methanol-Gasoline Blends," CRC Report No. 536, January 1984.
- Coordinating Research Council, Inc., "1982 CRC Fuel Rating Program: Road Octane Performance of Oxygenates in 1982 Model Cars," CRC Report Number 541, July 1985.
- Dean, John A., Lange's Handbook of Chemistry, 14th Edition, McGraw-Hill, Inc., New York, NY, 1992.
- Dorn, P., Muraio, A. M., and Herbstman, S., "The Properties and Performance of Modern Automotive Fuels," SAE Paper No. 861178, 1986.
- Ebersole, G. D., and Manning, F. S., "Engine Performance and Exhaust Emissions: Methanol versus Isooctane," SAE Paper No. 720692, 1972.
- Furey, Robert L., "Volatility Characteristics of Gasoline-Alcohol and Gasoline-Ether Fuel Blends," SAE Paper No. 852116, 1985.
- Furey, Robert L., "Trends in Gasoline Properties and Their Effects on Motor Vehicles," Air Pollution Control Association Paper GMR-5780 F&L-846, 1987.
- Furey, Robert L., and King, Jack B., "Emissions, Fuel Economy, and Driveability Effects of Methanol/Butanol/Gasoline Fuel Blends," SAE Paper No. 821188, 1982.

- Gabele, P. A., Baugh, O. J., and Black, F., "Characterization of Emissions From Vehicles Using Methanol and Methanol-Gasoline Blended Fuels," *Journal of the Air Pollution Control Association*, Vol. 35 (1985), pp. 1168-1175.
- Gatowski, J.A., Balles, E. N., Chun, K. M., Nelson, F. E., Ekchian, J.A., and Heywood, J.B., "Heat Release Analysis of Engine Pressure Data," Society of Automotive Engineers Paper 841359, 1984.
- Gautam, M., "Micro-Dilution Tunnel," Personal Communications, Department of Mechanical and Aerospace Engineering, West Virginia University, Morgantown, WV, 1994.
- Gautam, M., and Martin II, D.W., "Combustion Characteristics of Higher Alcohol/Gasoline Blends", *Fuel* (In-Review).
- Harrington, J. A., and Pilot, R. M., "Combustion and Emission Characteristics of Methanol," SAE Paper No. 750420, 1975.
- Hunwartz, I., "Modification of CFR Test Engine Unit to Determine Octane Numbers of Pure Alcohols and Gasoline-Alcohol Blends," SAE Paper No. 820002, 1982.
- Mays, M. A., "Exhaust and Evaporative Emission Studies with Fuels Containing Oxinol Blending Component and MTBE," EFOA Second Conference on Fuel Oxygenates, Rome, October 1987.
- Martin II, Daniel W., "Combustion and Emissions Characteristics of Higher Alcohol/Gasoline Blends," Masters Thesis, West Virginia University, Department of Mechanical and Aerospace Engineering, 1997.
- National Institute for Occupational Safety and Health, "Carcinogenicity of Acetaldehyde and Malonaldehyde, and Mutagenicity of Related Low-Molecular-Weight Aldehydes," Current Intelligence Bulletin 55, September, 1991.
- Owen, K., Coley, T., and Weaver, C. S., Automotive Fuels Reference Book, Second Edition, Society of Automotive Engineers, Inc., Warrendale, PA, 1995.
- Patel, K. S., Kumar, S., and Kwon, O. Y., "The Performance Characteristics of Indolene-MPHA Blends in a Spark Ignition Engine," SAE Paper No. 872068, 1987.
- Phillips 66, Certificate of Analysis of Unleaded Test Gas 96, Lot No. W-061A, Shipped 10/23/1995.
- Reddy, S. R., "Evaporative Emissions from Gasolines and Alcohol-Containing Gasolines with Closely Matched Volatilities," SAE Paper No. 861556, 1986.
- Schuetzle, D., Prater, T. J., and Anderson, R. D., "Characterization of Emissions From Methanol and Methanol/Gasoline Blended Fuels," SAE Paper No. 810430, 1981.

Yaccarino, P. A., "Hot Weather Driveability and Vapor-Lock Performance With Alcohol-Gasoline Blends," SAE Special Publication SP-638, 1985.